

# Inverse Cosmography: testing the effectiveness of cosmographic polynomials using machine learning

Cristian Zamora Muñoz<sup>a</sup> and Celia Escamilla-Rivera<sup>a</sup>

<sup>a</sup>Instituto de Ciencias Nucleares, Universidad Nacional Autónoma de México, Circuito Exterior C.U., A.P. 70-543, México D.F. 04510, México.

E-mail: [cristian.z.m@ciencias.unam.mx](mailto:cristian.z.m@ciencias.unam.mx), [celia.escamilla@nucleares.unam.mx](mailto:celia.escamilla@nucleares.unam.mx)

**Abstract.** Cosmography has been referred to as a solution to the *inverse scattering problem*, which is reasonable since it allows us to calculate cosmological bounds from data samplers by performing an expansion of the cosmological observables around present time. Nevertheless, this approach is not *properly* an inverse scattering solution since the method only circumvents the problem to fit the equation of state (EoS) parameters (model-dependent) by replacing it with their fit of its cosmographic parameters (with a polynomial series-dependence). Therefore, the question that we want to answer is: can we construct a *new cosmography approach* where the cosmodynamical parameters can be fitted and then employ them to analyse the kinematics via its *generic* cosmographic parameters? By all means, without experimenting with the traditional problem of truncation of the series that all cosmography proposals in the literature argue. In this work we present a solution to this question. A *generic* EoS depending solely on the form of  $f_i(z)$  and its derivative is found, where this function can be any polynomial (mimicking a dark energy-like term) that allow the dynamics of a specific cosmological density. We test our generic EoS with standard cosmological models and with polynomials proposals as Padé and Chebyshev approximants. All of them reproduce  $\Lambda$ CDM at  $z > 1$  between  $1-\sigma$ , but fail at lower observational redshift range. Interesting enough, a Padé (2,2) approximant has been considered inside a  $f(z)$ CDM-like model showing a transition in  $z = 1$ . Also, we found that this is not assured since models with these characteristics have degeneracy and truncation problems that experiment a divergence at this redshift limit. With a Chebyshev (2,1) approximant, here proposed, the divergence is not present for large redshifts. To explore our results, also we present a new supernovae sample trained via a deep learning tool called Recurrent-Bayesian (RNN+BNN) network that can solve problems as overfitting at lower redshifts and increase the density of data points in this region, which can help to discern between cosmographies at  $2-\sigma$  of precision.

---

## Contents

<b>1</b>	<b>Introduction</b>	<b>1</b>
<b>2</b>	<b>Inverse cosmography</b>	<b>3</b>
<b>3</b>	<b>The models</b>	<b>5</b>
3.1	Standard equations of state	5
3.1.1	$w$ -constant flat cosmological case ( $w$ CDM)	5
3.1.2	Chevallier-Polarski-Linder (CPL) case	6
3.1.3	Redshift squared (RS) case	6
3.2	$f(z)$ CDM Padé-like equations of state	6
3.3	$f(z)$ CDM Chebyshev-like equations of state	7
<b>4</b>	<b>The method</b>	<b>9</b>
4.1	Supernovae sampler	9
4.2	Recurrent plus Bayesian network (RNN+BNN)	9
<b>5</b>	<b>The results: How many cosmographic parameters?</b>	<b>11</b>
5.1	Standard equations of state	11
5.2	$f(z)$ CDM-like equations of state	15
<b>6</b>	<b>Discussion</b>	<b>19</b>
<b>A</b>	<b>Generic cosmographic parameters</b>	<b>23</b>
A.1	Chevallier-Polarski-Linder (CPL) case	23
A.2	Redshift squared (RS) case	24
A.3	$f(z)$ CDM Padé-like case	24
A.4	$f(z)$ CDM Chebyshev-like case	25

---

## 1 Introduction

To understand the cosmic accelerating evolution in a standard manner we often based our description of the Universe from a model-dependent way. This argument leads to a biased cosmic reconstruction of the dynamics of the universe, in where the cosmological parameters suffer from degeneracies problems or even cannot be well-tested with a good-fit convergence using observational samplers. Currently, these problems fall into the window of *cosmological tension parameter discussions*, like those of  $\sigma_8$  and  $H_0$  [1]. Strategies towards a model-independent analysis to relax these problems require the postulation a priori of the assumptions of homogeneity and isotropy in a scenario where the cosmic dynamic is independent of the energy densities. In this line of thought, the so-called cosmography has been proved to be an *optimized* method that can reconstruct the dynamical evolution of the cosmic acceleration (via a dark energy-like term) without assuming a specific cosmological model (see [2, 3], and references therein).

For many years, Cosmography has been referred to as an *inverse scattering approach*, which is reasonable since it allows us to calculate cosmological bounds directly from surveys by performing an expansion of the cosmological observables of interest around present time ( $a_{(z=0)} = a_0$ ). Nevertheless, Cosmography is not properly an inverse scattering approach since the method only circumvents the problem to fit the equation of state (EoS) parameters (with a model-dependency) by replacing it with their fit of its own cosmographic parameters (with a polynomial series-dependence). Therefore, the question that we want to solve is: can we construct a *new cosmography approach* where the cosmological parameters can be *dynamical* fitted as usual and then employ them to analyse the

*kinematics* via its cosmographic parameters? This without experimenting with the traditional problem of truncation of the series.

An interesting draw near to this question was addressed in [4], where a straightforward cosmography approach over the EoS was improved to test cosmological parametric versions of the dynamics of dark energy. In this approach, a homogeneous supernovae observational sampler was used to perform the statistical analysis of specific dark energy parameterisations to obtain *directly* the kinematics on the cosmographic parameters. The conclusion of this proposal lies in the fact that is possible to set constraints over the cosmographic parameter values using the cosmostatistics analyses of the dynamics imposed in the dark energy-like term. Also, the idea of using supernovae data<sup>1</sup> was with the aim to not taint statistical analyses with the Planck cosmic microwave background (CMB) temperature data, since this survey is best fitted with a  $\Lambda$ CDM model that is in mild tension with constraints from dynamical data probes. Some cosmography proposals available in the literature perform a test with this latter sampler, which is misleading to consider it since this approach is unlikely to reveal any new physics beyond an improved  $\Lambda$ CDM with higher corrections. And these corrections are directly linked to low redshift data precision –also in the context of a Bayesian approach–.

According to the above issues and with the results in [4], our proposal in this paper consists in an *inverse technique* that can obtain a *generic* equation of state without assuming directly a cosmographic series. Therefore, we relax two inherent cosmography problems such as

- (i) The study of the dark energy dynamics (without a cosmological constant  $\Lambda$ ) by proposing standard Taylor series or suitable Padé or Chebyshev polynomials evolving with a cold dark matter (CDM) fluid.
- (ii) The calculations of the cosmographic parameters using (i) without truncation problems over the series/polynomials proposed.

As an extension of this approach, and in order to work with a homogeneous data sampler at low redshift, in [5] was proposed a novel computational tool based in machine learning (ML) for supernovae, called Recurrent-Bayesian Neural Networks (RNN+BNN). A deep learning architecture, inside this ML, can develop a trained homogeneous supernovae sampler in where the resulting dynamics of dark energy could lead to the necessity of another cosmological model different from  $\Lambda$ CDM. In such a scenario, our *inverse cosmography approach* can fit statistically very well since is not necessary to consider higher-order corrections of the cosmography series to obtain a convergence best fit in comparison to the standard dark energy EoSs. Also, using training deep learning data for a homogeneous sample as supernovae show, from a Bayesian point of view, better evidence without dealing with the degeneracy of the models at third order of the series. This aspect usually appears when a combination of surveys is considered [6]. While in the near future, high-redshift spectroscopy surveys [7–9] or Gravitational Waves surveys [10, 11] will provide accurate data in redshifts of  $2 < z < 5$ , our present deep learning result [5] allows to acquire more density of precise data of one species, the modulus distance, in redshifts range  $0.01 < z < 4$ .

To achieve our goal, this paper is organised as follows: in Sec.2 we describe the standard background cosmography in order to get the inverse cosmography. In Sec.3 we present three standard cases for the EoS with dark energy-like terms  $f(z)$  as cosmological fluids. Also, we introduce the description of the  $f(z)$ CDM model using Padé and Chebyshev polynomial approaches. We calculate the EoS derived from the inverse cosmography and their cosmographic parameters at present time up to fourth order in the series. In Sec.4 we introduce the RNN+BNN architecture to train the supernovae Pantheon sampler [5]. The recipe to perform this training is also explained. In Sec.5 we perform statistical analyses for the models considered and we show the information criteria results that allow us to carry out model selection. In Sec.6 we will discuss the main results. To make the treatment comprehensive, in the Appendix we present the exact expressions for the cosmographic parameters for each model under consideration.

---

<sup>1</sup>In [4] was used the Joint Lightcurve Analysis (JLA) sampler, which has extra nuisance parameters, related to the color  $\alpha$  and stretch  $\beta$  luminosity, in comparison to the recent Pantheon sampler. In this paper we focus in using the latter sampler by setting  $\alpha = \beta = 0$ .

## 2 Inverse cosmography

We start by describing the standard cosmography equations. As it follows, this approach consider a Taylor-like expansion of the scale factor around  $z = 0$ , which is the only parameter that can measure the Hubble flow according to the cosmological principle, therefore we can write

$$a(t) = 1 + \sum_{n=1}^{\infty} \frac{1}{n!} \left. \frac{d^n a}{dt^n} \right|_{t=t_0} (t - t_0)^n, \quad (2.1)$$

where the Hubble, deceleration, jerk and snap parameters give information of the late universe and are defined respectively as:

$$H(t) \equiv \frac{1}{a} \frac{da}{dt}, \quad q(t) \equiv -\frac{1}{aH^2} \frac{d^2 a}{dt^2}, \quad j(t) \equiv \frac{1}{aH^3} \frac{d^3 a}{dt^3}, \quad s(t) \equiv \frac{1}{aH^4} \frac{d^4 a}{dt^4}. \quad (2.2)$$

Extra cosmographic parameters has longer definitions which involve high order derivatives of  $H(z)$  in a sequence given by:  $\dot{a} = aH$ ,  $\ddot{a} = -qaH^2$ ,  $\dddot{a} = jaH^3$ ,  $d^4 a/dt^4 = saH^4$ , and  $d^5 a/dt^5 = laH^5$ .

The signs of each cosmographic parameter gives information about the cosmic kinetic scenario: the sign of the deceleration parameter  $q$  indicates whether the universe is accelerating (negative sign) or decelerating (positive sign), the sign of  $j$  determines the change of the universe dynamics and the value of  $s$  is necessary to discriminate between evolving dark energy or  $\Lambda$ <sup>2</sup>. From here we notice that divergences in Taylor series are observed at  $z > 1$ , since the expansion is performed around  $z = 0$ , as a consequence of the convergence radius. These cosmographic parameters are essential since their character over the sign immediately shows kinematic of the universe. Moreover, all of them are not observable quantities, therefore we require to perform a data fit over a specific model rewritten in terms of these parameters using astrophysical observations.

Until this point, we can relax the degeneracy problem among cosmological models—certainly, with the Cosmological Principle as the backbone of this approach—, and in some manner, the hypothesis model(s) under testing will be the best one(s) once we perform the corresponding statistical cosmology over it(them). The consequence of using this approach is the high degeneracy and divergence on the terms related to the cosmographic parameters. The current arguments to defend this method still remains in the idea of *more data, better precision* and the divergence of the series can be alleviated per se. Even with these ideas, cosmography remains unsuitable if we continue to study it with the following methodology:

1. Propose a Taylor (polynomial) series for the Hubble parameter around present time.
2. Write the luminosity distance as a function of the redshift.
3. Confront the *cosmographic parameters* of the series with the current astrophysical samplers.
4. Set the bounds on the cosmographic parameters with several kinds of surveys.

The final task of this methodology remains in the fact that kinematics of the universe can be understood by setting limits of the standard cosmography using not only Taylor series [13], but also Padé and Chebyshev polynomials to parameterise cosmic distances and solve the problem of the error propagation over the statistical test [14, 15]. More interesting approaches have been done towards a *cosmography equation of state* [16] or to link the late universe expansion with the early universe via a *parametric cosmography* [17]. However, none of them have yet set a *non-stop*-rule on the proposed cosmographic series with the use of combined observational samplers. Over the general ideas until now, a low order of the series expansion will generate numerical values within the error propagation of the cosmographic parameters, while a high order of the propagation can be done in a large statistical region of these parameters. This transition of redshift regions can be enough treated by considering different data samplers. At the end, the series will be only *well truncated* depending on the quality of the measurements, and even then, systematics characteristics remain with the wrong results.

<sup>2</sup>An analogous approach of this *snap* parameter is the  $O_m$ -diagnostic at second order [12].

All these proposals express the concern about finding not only a model-independent scenario, but the endless loop tests of different kinds of polynomials in order to found a well-fitted description of the kinematics of the universe. In this direction, in [4] was proposed a mathematical expression to obtain the EoS for a specific dynamical model. This expression allows us to obtain the cosmographic parameters without assuming *directly* a cosmography-dependent polynomial series over them. Along the rest of this paper, we are going to refer to this approach as *inverse cosmography*.

With the inverse cosmography approach, we can obtain directly the cosmographic parameters values by only fitting a specific function that can replace the standard dark energy-like term without dealing with the mentioned problems, i.e. we can constrain directly the cosmological parameters for the model and use them to compute the cosmographic parameters, e.g  $q(z)$  and  $j(z)$  (also  $q_0$  and  $j_0$ ) without considering higher corrections over them [15] or perform a change of variables over the redshift to avoid divergences.

To start with the derivation of the inverse cosmography, we start as usual: with the spatial flatness hypothesis on the Hubble function as

$$\left(\frac{H(z)}{H_0}\right)^2 = \Omega_k(1+z)^2 + \Omega_m(1+z)^3 + \Omega_r(1+z)^4 + \Omega_i f_i(z), \quad (2.3)$$

where curvature  $\Omega_k$  and radiation  $\Omega_r$  contributions can be neglected in a late universe scenario, and the density closure relation is that  $\Omega_m + \Omega_i = 1$ . The term  $\Omega_i$  is related with the standard description of the current universe dynamics once the form of  $f(z)$  is given. From here we are going to refer  $i = \Lambda$  as standard dark energy scenarios and  $i = p$  as polynomial scenarios with their Hubble flow function given by, respectively

$$\left(\frac{H(z)}{H_0}\right)^2 = \Omega_m(1+z)^3 + \Omega_\Lambda f_\Lambda(z), \quad (2.4)$$

$$\left(\frac{H(z)}{H_0}\right)^2 = \Omega_m(1+z)^3 + \Omega_p f_p(z), \quad (2.5)$$

where  $\Omega_\Lambda = 1 - \Omega_m$  and  $\Omega_p$  is a CDM-*fluid* related to the polynomial case<sup>3</sup>.

However, this approach requires a fiducial model, e.g. we can assume a flat quiescence model or a dynamical dark energy model. Therefore, we can write a *generic* expression for the cosmological EoS in where we do not impose any form of dark energy-like  $\Omega_i$  by formally solve (2.3) to obtain

$$w(z) = -1 + \frac{1}{3}(1+z)\frac{f_i(z)'}{f_i(z)}, \quad (2.6)$$

where the prime denotes  $d/dz$ . Notice that this *generic EoS* depends solely on the form of  $f_i(z)$ . This is an interesting result since we obtain an EoS that only requires a function form of  $z$  and its derivative, e.g this function can be any polynomial at hand that allow the dynamics of a specific cosmological density.

Following the inverse cosmography idea, we can use the definitions (2.2) and (2.6) with the chain rule  $\dot{\phantom{x}} = d/dt = -(1+z)H(z)d/dz$ , to obtain our new set of cosmographic parameters in terms  $H(z)$  and its derivatives:

$$q(z) = -1 + \frac{1}{2}(1+z)\frac{[H(z)^2]'}{H(z)^2}, \quad (2.7)$$

$$j(z) = \frac{1}{2}(1+z)^2\frac{[H(z)^2]''}{H(z)^2} - (1+z)\frac{[H(z)^2]'}{H(z)^2} + 1, \quad (2.8)$$

$$s(z) = -\frac{1}{6}(1+z)^3\frac{[H(z)^2]'''}{H(z)^2} + \frac{1}{2}(1+z)^2\frac{[H(z)^2]''}{H(z)^2} + (1+z)\frac{[H(z)^2]'}{H(z)^2} - 1. \quad (2.9)$$

---

<sup>3</sup>This can be seen as the replace of the  $\Lambda$ -fluid term as it was stated in [17].

By solving and evaluate them at  $z = 0$  we get the usual cosmographic series

$$H(z) = H_0 + \frac{dH}{dz} \Big|_{z=0} z + \frac{1}{2!} \frac{d^2 H}{dz^2} \Big|_{z=0} z^2 + \frac{1}{3!} \frac{d^3 H}{dz^3} \Big|_{z=0} z^3 + \dots \quad (2.10)$$

Similar expressions can be calculated by expressing everything in terms of the function normalised by the Hubble constant,  $E(z) = H(z)/H_0$  and its derivatives. Nonetheless, the information we can obtain from this is exactly equivalent.

### 3 The models

In this work we analyse three standard dark energy scenarios and two polynomial approaches to found directly their corresponding EoS using our generic equation (2.6). The first subsection is devoted to the standard  $w$ CDM model and Taylor-like parameterisations as Chevallier-Polarsky-Linder (CPL) and Redshift Squared (RS). In the second subsection the scenario presented will be a  $f(z)$ CDM-like approach based in Padé (2,2) and Chebyshev (2,1) polynomial expressions. To make the treatment comprehensive, in the following sections we present the cosmographic parameters for each model at present time. In the Appendix we develop the exact expressions for the general cosmographic parameters for each model under consideration.

#### 3.1 Standard equations of state

As it is standard when we have to deal with a specific form dark energy with

$$f_\Lambda(z) = \exp \left[ 3 \int_0^z \frac{1 + w_\Lambda(\tilde{z})}{1 + \tilde{z}} d\tilde{z} \right], \quad (3.1)$$

there is not a theoretical consensus ad idem to choose the best  $w_\Lambda(z)$ , only an optimal form that can be cosmologically viable, e.g. for quiescence models ( $w_\Lambda = \text{constant}$ ), we have  $f_\Lambda(z) = (1+z)^{3(1+w_\Lambda)}$ . For a cosmological constant if  $w_\Lambda = -1$  then  $f_\Lambda = 1$ . Constrictions over the free parameters in the models is a useful way to compare the relative performance of several kinds of surveys to reconstruct the cosmic expansion [18]. Nonetheless, a generic form of  $w_\Lambda$  remains unknown.

By using (2.7)-(2.8)-(2.9), we can easily derive the cosmographic parameters without dealing with higher derivatives for the solution of  $H(z)$ . Also, the cosmographic expressions obtained will show a relation between the kinematics and the dynamics of the universe. For this task, we are going to consider the following models:

##### 3.1.1 $w$ -constant flat cosmological case ( $w$ CDM)

This model can be modelled by:

$$\left( \frac{H(z)}{H_0} \right)^2 = \Omega_m (1+z)^3 + \Omega_\Lambda (1+z)^{3(1+w)}, \quad (3.2)$$

where  $\Omega_m$  is the present matter density and  $\Omega_\Lambda = (1 - \Omega_m)$  the dark energy density. According to this model, and using our inverse cosmographic parameters defined above, we compute the following cosmographic parameters:

$$q(z) = \frac{1}{2} \left[ \frac{3w\Omega_m}{(\Omega_m - 1)(z+1)^{3w} - \Omega_m} + 3w + 1 \right], \quad (3.3)$$

$$j(z) = \frac{[9w(w+1) + 2](\Omega_m - 1)(z+1)^{3w} - 2\Omega_m}{2(\Omega_m - 1)(z+1)^{3w} - 2\Omega_m}, \quad (3.4)$$

$$s(z) = - \frac{[9w(w+1) + 2](\Omega_m - 1)(w-z)(z+1)^{3w} + 2z\Omega_m}{2(z+1)[(\Omega_m - 1)(z+1)^{3w} - \Omega_m]}, \quad (3.5)$$

where we can notice that for dust  $w = 0$ :  $q = 1/2$ ,  $j = 1$  and  $s = 0$  holds for any redshift. If we consider the evaluation of these parameters at  $z = 0$  and for a particular value of  $w_\Lambda = -1$  we recover the standard  $\Lambda$ CDM scenario:  $2q_0 + j_0 + s_0 = 2(\Omega_m - 1)$ .

### 3.1.2 Chevallier-Polarski-Linder (CPL) case

The evolution for this model [19, 20] can be represented by two parameters that exhibit the present value of the EoS  $w_0$  and its overall time evolution  $w_a$ :

$$\left(\frac{H(z)}{H_0}\right)^2 = \Omega_m(1+z)^3 + \Omega_\Lambda(1+z)^{3(1+w_0+w_a)}e^{-\left(\frac{3w_a z}{1+z}\right)}. \quad (3.6)$$

Following the above prescription, we can obtain the following cosmographic parameters at present time:

$$q_0 = \frac{(3w_0 + 1)(\Omega_m - 1) - \Omega_m}{2(\Omega_m - 1) - 2\Omega_m}, \quad (3.7)$$

$$j_0 = \frac{1}{2} \left[ -(3w_a + 2)(\Omega_m - 1) - 9w_0^2(\Omega_m - 1) - 9w_0(\Omega_m - 1) + 2\Omega_m \right], \quad (3.8)$$

$$s_0 = \frac{[(-9w_0 - 2)w_a - w_0(9w_0(w_0 + 1) + 2)](\Omega_m - 1)}{2(\Omega_m - 1) - 2\Omega_m}. \quad (3.9)$$

### 3.1.3 Redshift squared (RS) case

This model [21] relax CPL parameterisation divergency in low redshift regions and can be well-behaved at  $z \rightarrow -1$ . The evolution of this model is given by

$$\left(\frac{H(z)}{H_0}\right)^2 = \Omega_m(1+z)^3 + (1 - \Omega_m)(1+z)^{3(1+w_0)}(1+z^2)^{\frac{3w_a}{2}}. \quad (3.10)$$

For this case the cosmographic parameters at present time are

$$q_0 = \frac{1}{2} [3(\Omega_m - (w_0 + 1)(\Omega_m - 1)) - 2], \quad (3.11)$$

$$j_0 = \frac{1}{2} [2 - 3(w_a + 3w_0(w_0 + 1))(\Omega_m - 1)], \quad (3.12)$$

$$s_0 = -\frac{1}{2} [(-9w_0 - 6)w_a - w_0(9w_0(w_0 + 1) + 2)](\Omega_m - 1). \quad (3.13)$$

$$(3.14)$$

## 3.2 $f(z)$ CDM Padé-like equations of state

The Padé approximation for cosmographic analyses [22] has showed to have larger convergence radius in comparison to Taylor-like series, as the ones described above, and it is proving to be an optimal choice to extent the analysis to higher redshifts as:

$$P_{(n,m)}(z) = \frac{\sum_{i=0}^n a_i z^i}{1 + \sum_{j=1}^m b_j z^j}, \quad (3.15)$$

where the Padé approximant  $P_{(n,m)}$  of order  $n/m$ , define the ratio between two standard Taylor-like series as  $f(z) = \sum_{i=0}^{\infty} a_i z^i$ . In the latter reference was presented a possibility to extent the analysis up to  $z \sim 6$  for a Padé approximation of order (2,2). In our inverse cosmography approach we are going to consider this order on the polynomial since our deep learning training data is up to this redshift range. Following the proposal in [17], but taking into account the full definition for the Padé approximant we write a new background evolution as

$$f_p(z) = \frac{P_0 + P_1 z + P_2 z^2}{1 + Q_1 z + Q_2 z^2}, \quad \rightarrow \quad P_{(2,2)} = \frac{H(z)}{H_0} = \frac{1 + P_1 z + P_2 z^2}{1 + Q_1 z + Q_2 z^2}, \quad (3.16)$$



where in the standard cosmography approach, each coefficient of the polynomial is a function that depends on the cosmographic parameters [6], making the analysis a loop problem because of the model-dependent on every of them.

At this point, we can apply our inverse cosmography approach over a  $f(z)$ CDM-like model, where  $\Lambda$  is replaced by a Padé (2,2) polynomial in (2.5) and then obtain its characteristic EoS via (2.6)

$$w(z)_{\text{Padé}} = -1 + \frac{(z+1) [P_1 (1 - Q_2 z^2) + P_2 z (Q_1 z + 2) - P_0 (2Q_2 z + Q_1)]}{3 [z (P_2 z + P_1) + P_0] (z (Q_2 z + Q_1) + 1)}, \quad (3.17)$$

from where if we consider  $P_0 = 1$  we obtain the EoS for Padé (2,2). This term in the denominator will be important from a computational point of view, since will allow us to integrate without having divergencies at low redshift (see Sec.5.2). Notice how we recover  $\Lambda$ CDM at larger redshifts. According to this proposal and consider the Padé (2,2) (3.16) as  $f_p(z)$  in (2.5), we can compute the corresponding cosmographic parameters at present time using again (2.7)-(2.8)-(2.9):

$$q_0 = \frac{3\Omega_m + \Omega_p (-P_1 - Q_1)}{2(\Omega_m + \Omega_p)} - 1, \quad (3.18)$$

$$j_0 = \frac{\Omega_p [P_1 (Q_1 + 1) + P_2 + Q_1 (Q_1 + 1) - Q_2]}{\Omega_m + \Omega_p} + 1, \quad (3.19)$$

$$s_0 = 1 - \frac{\Omega_m + \Omega_p [-(P_1 + 1)Q_1 - P_2Q_1 + Q_1 [Q_1 (-(P_1 + Q_1)) - Q_1] + Q_2 (P_1 + 2Q_1) + Q_2]}{\Omega_m + \Omega_p} - \frac{(P_1 + P_2)\Omega_p}{\Omega_m + \Omega_p}. \quad (3.20)$$

From these latter equations we see that for the case with  $P_i = Q_i = 0$ , we recover a  $\Lambda$ CDM EoS and its respectively cosmographic parameters at present time  $q_0 = -1$ ,  $j_0 = 1$ ,  $s_0 = 0$ . This without calibrating the luminosity distance as it is usually done in regards to *standard cosmography*.

### 3.3 $f(z)$ CDM Chebyshev-like equations of state

In [15] was proposed a method to optimize the standard technique of rational polynomials and consists in defining the  $(n, m)$  rational Chebyshev approximant with a coefficient  $b_0 \neq 0$  as

$$R_{(n,m)}(z) = \frac{\sum_{i=0}^n a_i T_i(z)}{1 + \sum_{j=1}^m b_j T_j(z)}. \quad (3.21)$$

Applying a similar procedure used to obtain the Padé approximants, we can compute the background evolution with a rational Chebyshev  $R_{(2,1)}$  as

$$f_p(z) = \frac{a_0 + a_1 z + 2a_2 z^2 - a_2}{1 + b_1 z}, \quad \rightarrow \quad R_{(2,1)} = \frac{H(z)}{H_0} = \frac{a_3 + a_1 z + 2a_2 z^2}{1 + b_1 z}, \quad (3.22)$$

where  $a_3 = a_0 - a_2$ . Once again, in the standard cosmography approach, each coefficient  $a_i$  and  $b_i$  is a function that depends solely on the cosmographic parameters [15]. To relax the model-dependent loop problem, we calculate, as we did in the Padé case, our inverse cosmography approach as  $f(z)$ CDM-like model, where  $\Lambda$  is replaced now by the rational Chebyshev  $R_{(2,1)}$  in (2.5) and then obtain its characteristic EoS via (2.6)

$$w(z)_{\text{Chebyshev}} = -1 + \frac{[2a_2 z (b_1 z + 2) - a_3 b_1 + a_1] (z + 1)}{3 (z (2a_2 z + a_1) + a_3) (b_1 z + 1)}, \quad (3.23)$$



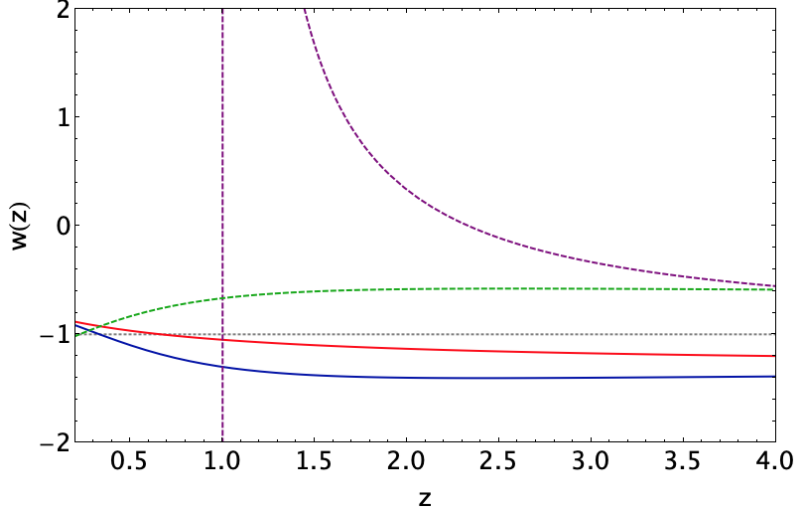


**Figure 1:** Equation of state for the standard cosmological models Sec.(3.1) and  $f(z)$ CDM cosmological models Secs.(3.2-3.3). For this evolution, the  $\Lambda$ CDM (grey dotted line), the standard models CPL and RS (red and blue solid lines, respectively) and the Padé (2,2) and Chebyshev (2,1) (purple and green dashed lines, respectively) are assumed with negative values of  $w_i$ , and positive values for all the free coefficients in the polynomials.

from where  $a_3 = a_1/b_1$  to avoid any divergencies. We will perform a change of variable over  $a_0$  once we integrate this EoS in Sec.5.2, in this manner we preserved the same expression for Chebyshev approximant (3.22). We recover again  $\Lambda$ CDM at larger redshifts. Now, we can compute the corresponding cosmographic parameters at present time using (2.7)-(2.8)-(2.9):

$$q_0 = \frac{(a_1 - a_3 b_1) \Omega_p + 3\Omega_m}{2(a_3 \Omega_p + \Omega_m)} - 1, \quad (3.24)$$

$$j_0 = \frac{[a_1(-b_1 - 1) + a_3 b_1(b_1 + 1) + 2a_2 + a_3] \Omega_p + \Omega_m}{a_3 \Omega_p + \Omega_m}, \quad (3.25)$$

$$s_0 = \frac{[-a_1(b_1 + 1) + a_3 b_1(b_1 + 1) + 2a_2 + a_3] \Omega_p + \Omega_m}{a_3 \Omega_p + \Omega_m}. \quad (3.26)$$

At this point, in the case with  $a_1 = a_2 = a_3 = 0$  and  $b_1 = 0$ , we obtain a cosmology with a universe that is decelerating at present time and with a preference for a cosmological constant. Noteworthy, this theoretical analysis allows us to see that the cosmography is sensible to the values of the coefficient for this polynomial and present an anti-correlation between the cosmographic parameters. Notice that this result has been discussed in [17] after an exhaustive statistical analysis with data sets. We obtain the same without considering cosmostatistics tools yet. We verify our arguments in Sec.5 and extend them with deep learning methods.

In Fig. 1, a comparison between our EoS is shown. According to the values considered for each free coefficients in the models, our analyses show a disagreement with [23] and [17]<sup>4</sup> since while the standard models behave as it is expected, the polynomial choices show a quintessence behaviour for  $z > 1$ . Notice how both polynomial asymptotically approach each other near to  $z \sim 4$  (our optimal redshift to perform the deep learning training, as we shall see below). Also, in the latter reference was suggested that Padé (2,2) can be a good choice in redshift regions  $z < 1$ , but from its EoS we obtain that at  $z = 1$  there is a divergence. So the *link* between their toy model and the Padé approach is never reached. The reason for their results lies in the use of biased best fits that experiment truncation problems to test this toy model.

<sup>4</sup>In this reference was used the same best fits values of [23].

## 4 The method

In [5] was proposed a novel deep learning architecture in order to study the evolution of dark energy models from an EoS point of view. The goal was to combine two architectures: the Recurrent Neural Networks (RNN) and the Bayesian Neural Networks (BNN), from now on we refer to this method as RNN+BNN network. Without being extremely thorough in describing the computational method developed in this research, in this paper we devoted our objective in describe the methodology to implement our inverse cosmography in this architecture. A summary of the importance of this computational methodology is that we can train a neural network with their own confidence regions for specific homogeneous data. Additionally, RNN+BNN network minimizes the computational batch of expensive codes for dark energy models and probe the deviation from the  $\Lambda$ CDM scenario at large redshifts for a supernovae trained sampler. Therefore, in this section we start by describing the supernovae sampler used to train the network. Afterward, we describe the RNN+BNN architecture employed to implement the inverse cosmography.

### 4.1 Supernovae sampler

We choose to build the RNN+BNN network by training the Pantheon supernovae sampler that consist in 40 bins [26] compressed in a redshift range [0.01, 2.3]. Type Ia supernovae can give determinations of the distance modulus  $\mu$ , whose theoretical prediction is related to the luminosity distance  $d_L$ . As we are consider spatial flatness, the  $d_L$  is related to the comoving distance  $D$  as  $d_L(z) = cH_0^{-1}(1+z)D(z)$ , where  $c$  is the speed of light. From here we can compute the normalised Hubble function  $H(z)/H_0$  by taking the inverse of the derivative of  $D(z)$  with respect to  $z$

$$D(z) = \int_0^z H_0 d\tilde{z}/H(\tilde{z}), \quad (4.1)$$

where  $H_0$  is the Hubble constant consider as a prior value to normalise  $D(z)$ .

### 4.2 Recurrent plus Bayesian network (RNN+BNN)

To perform the deep learning training, we follow the methodology given in [5]. Our finals steps will define the process of how we can deal with the cosmography described in the above sections.

- Training the supernovae data with RNN+BNN architecture
  - Step 1. Construction of the neural network. For RNN we choose a Tanh activation function with 8 hyperparameters: Size=4, Epochs=100, Layers=1, Neurons=100, Bathsize=10. And a variational dropout composed by an input  $z$ , a hidden state  $h$  and an output  $\mu(z)$ . A diagram of this architecture was developed in [5], also it demonstrated why a Tahn function is adequate to train supernovae data from a Bayesian point of view<sup>5</sup>.
  - Step 2. Organising the data. We ordering the Pantheon data from higher to low redshift with a choice of a number of steps  $n = 4$ .
  - Step 3. Calculation of the confidence errors via BNN. Due to the easiness of neural networks to overfit, it is important to choose a mode of regularisation. BNN allows our algorithm to calculate errors via a regularisation method. Our dropout has the following parameter: the probability to dropped the input is 0, this is because after testing several times, we found that our models could not be training with input dropout due to the lost of information. Since the cost function is MSE type (see Figure 2, bottom plot) we can use Adam optimizer.
  - Step 4. Results from the training. After the training, we read the model and apply 500 times the same dropout to our initial model. The predicted sampler with the above characteristics consist of 1810 data points in a redshift range of [0.01 – 4.0]. See Figure 2, top plot).

---

<sup>5</sup>As a summary of this process, several trainings with different activation functions were analised, moreover, just two of them gave a physical trend for the supernovae modulus distance  $\mu(z)$ , and between these, Tanh function has the better Bayesian evidence in  $2\text{-}\sigma$  C.L. A RNN+BNN architecture portrait of these steps is given in Fig. 1 in [5].

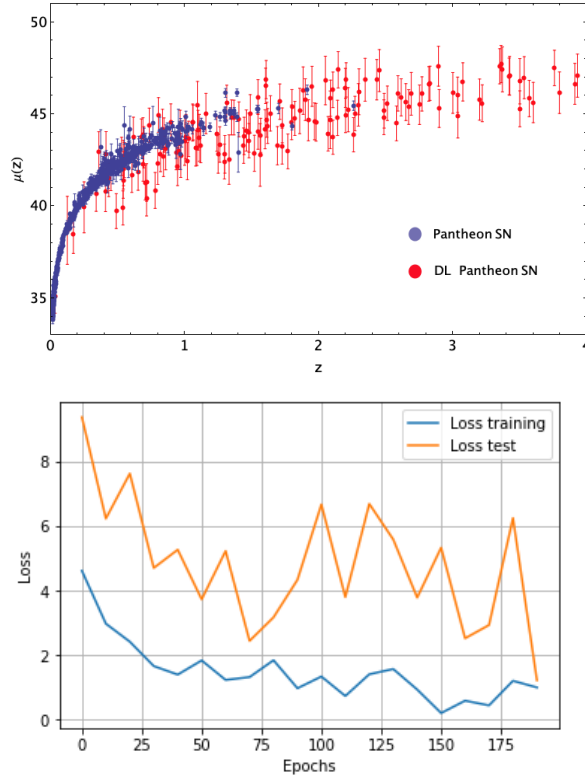


**Figure 2:** Top: Deep learning training for Pantheon sampler up to  $z = 4$ . The error bars represent the 1- $\sigma$  C.C. The Pantheon observational data is given by the purple dots and the training RNN+BNN supernovae data is given by the red points. Bottom: Loss versus epochs plot for the training RNN+BNN supernovae data. This training was performed using a Tanh as activation function, which shows a better Bayesian evidence according to [5].

- Inverse Cosmography in Deep Learning RNN+BNN:
  - Step 5. Compute  $\mu(z)$  for each cosmological model. We obtain  $\mu$  by using the cosmological models described in Sec.3 and integrating them to obtain  $H(z)/H_0$ . At this step we increase the number of epochs up to 1000.
  - Step 6. Calculate the best fits cosmographic parameters. We modified the publicly version codes CLASS<sup>6</sup> and Monte Python<sup>7</sup> to constrain the models from Sec.3 using RNN+BNN Pantheon sampler from the Step 4 obtained and add them in Step 5.

We notice that this algorithm can easily perform the fit of cosmological models with independent model priors. The only restriction is that our choice of activation function can be viewed as a *choice of a prior* since it is relevant in regions where the training data is sparse or even non-existent and the resulting trained supernovae sampler depends on this choice. Nevertheless, this is a *physical prior* selection since Tanh activation function can exhibit a behaviour similar to SNeIa's, where the observed differences in their peak luminosities are near correlated with observed differences in the shapes of their light curves. Also this is supported by high Bayesian evidence [5].

<sup>6</sup>[https://github.com/lesgourg/class\\_public](https://github.com/lesgourg/class_public)

<sup>7</sup>[https://github.com/baudren/montepython\\_public](https://github.com/baudren/montepython_public)

Parameters	Prior CPL (uniform)	Parameters	Prior RS (uniform)
$\Omega_m$	[0.25,0.35]	$\Omega_m$	[0.25,0.34]
$\Omega_\Lambda$	[0.65,0.75]	$\Omega_\Lambda$	[0.66,0.75]
$H_0$	[64,74.4]	$H_0$	[64.8,73.7]
M	[-19.5,-19.2]	M	[-19.5,-19.2]
$w_0$	[-1.31,0.53]	$w_0$	[-1.26,-0.64]
$w_a$	[-0.26,0.94]	$w_a$	[-1.36,0.46]

**Table 1:** Ranges of the model parameters considered in this paper. The *left panel* [*right panel*] indicates the priors for CPL (3.6) [RS (3.10)] models .

## 5 The results: How many cosmographic parameters?

In this section we present the results for the information criteria AIC and BIC [24] to compare our cosmological models and select the *best* one in comparison to the standard  $\Lambda$ CDM from an inverse cosmography point of view.

In agreement with the information criteria idea, we compute the logarithm of the Bayes factor between two models  $\mathcal{B}_{ij} = \mathcal{E}_i/\mathcal{E}_j$ , where the reference model ( $\mathcal{E}_i$ ) with the highest evidence is the  $\Lambda$ CDM model and without a flat prior over  $H_0$ . We apply our modified version of the MCEvidence code<sup>8</sup> since it calculates the bayesian evolving from MCMC chains employed to fit the cosmological parameters instead of fitting the cosmographic parameters as it is usually done. We based our discretisation on Jeffreys’s scale [25]: if  $\ln B_{ij} < 1$  there is no significant preference for  $\Lambda$ CDM (or weak); if  $1 < \ln B_{ij} < 2.5$  the preference is substantial (or positive); if  $2.5 < \ln B_{ij} < 5$  it is strong; if  $\ln B_{ij} > 5$  it is decisive (or very strong).

In order to develop our Bayesian analyses, we are going to consider the following steps:

- (i) We are using the three kinds of samplers: Pantheon observational, our RNN+BNN trained supernovae sample (DL) and the join of these samplers (Pantheon+DL), to perform the fitting of the cosmological parameters.
- (ii) By statistical inference analyses, we will select the best model in comparison to  $\Lambda$ CDM.
- (iii) Using the best fits values we can compute our cosmographic parameters without any degeneracy and truncation problems using our exact solutions given en Sec.3 for each of the cosmological models. We emphasize this step since all the methodologies in the literature impose a minimum requirement to obtain a positive luminosity distance or positive  $H^2$  in a redshift range  $0 < z/(1+z) < 1$ .

### 5.1 Standard equations of state

- Case  $\Lambda$ CDM. We present our statistical results using Eqs.(3.2)-(3.3)-(3.4) and the steps described in (i)-(ii)-(iii) above. For this model we notice that our trained data overlaps the observational results and show a better confidence contour at  $1-\sigma$  (see Figure 3). Also, we recover the standard cosmographic parameters values at larger redshift (up to  $z = 4$ ) as it is shown in Figure 4 for the three samplers.
- Case CPL. We present our statistical results using Eqs.(3.6)-(3.7)-(3.8) and the steps described in (i)-(ii)-(iii) above. For this model we notice that our trained data overlaps the observational results in parameters spaces where there is not dependence of the cosmological parameters. Suggesting that CPL is not a good option for  $z > 2.3$ , the observational cutoff of Pantheon sampler. When the samplers are combined, the C.C are better with a correlation of the cosmological

<sup>8</sup><https://github.com/yabebalFantaye/MCEvidence>

Parameters	Prior Padé (uniform)	Parameters	Prior Chebyshev (uniform)
$\Omega_m$	[0.09,0.81]	$\Omega_m$	[0.09,0.89]
$\Omega_\Lambda$	[0.19,0.91]	$\Omega_\Lambda$	[0.10,0.90]
$M$	[-19.5,-19.3]	$M$	[-19.5,-19.3]
$P_1$	[0.0,1.0]	$a_1$	[-0.15,107]
$P_2$	[-0.2,0.22]	$a_2$	[-0.72,0.61]
$Q_1$	[-0.3,3.0]	$b_1$	[-12.2,18.6]
$Q_2$	[-0.2,0.22]	$a_3$	[-0.01,5.75]

**Table 2:** Ranges of the model parameters considered in this paper. The *left panel* [*right panel*] indicates the priors for Padé (3.16) [Chebyshev (3.22)] models.

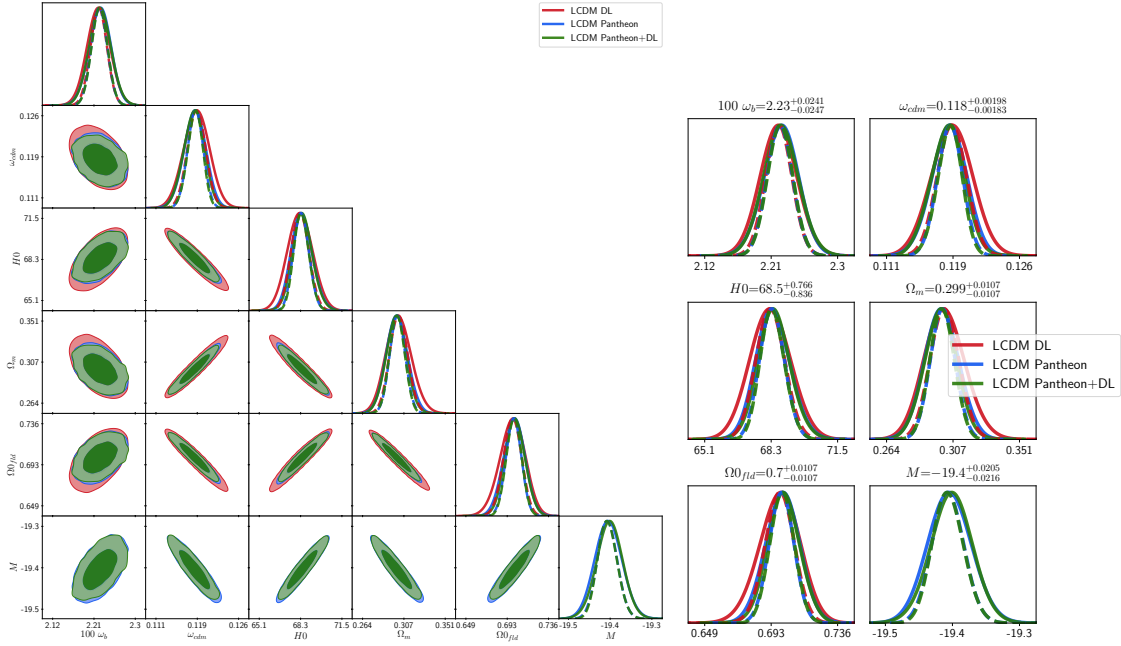


**Figure 3:** *Left:* Confidence contours, *Right:* Posterior, for  $\Lambda$ CDM model using Pantheon observational (blue), our RNN+BNN trained supernovae sample (DL) (red) and the join of these samplers (Pantheon+DL) (green).

**Table 3:** Best fits values for  $\Lambda$ CDM model using Pantheon sampler.

Parameters	Best-fit	mean $\pm\sigma$	95% lower	95% upper
100 $w_b$	2.224	$2.226^{+0.024}_{-0.025}$	2.177	2.274
$w_{cdm}$	0.118	$0.118^{+0.002}_{-0.002}$	0.114	0.122
$M$	-19.4	$-19.4^{+0.022}_{-0.023}$	-19.44	-19.35
$H_0$	68.36	$68.43^{+0.81}_{-0.88}$	66.8	70.11
$\Omega_m$	0.301	$0.300^{+0.011}_{-0.011}$	0.2776	0.322
$\Omega_\Lambda$	0.700	$0.670^{+0.011}_{-0.011}$	0.678	0.722

parameters at 1- $\sigma$  (see Figure 5). We compute the standard cosmographic parameters values at larger redshift (up to  $z = 4$ ) as it is shown in Figure 6 for the three samplers. Notice that our RNN+BNN supernovae sample does not prefer CPL model at low redshift, indicating that

**Table 4:** Best fits values for  $\Lambda$ CDM model using RNN+BNN supernovae (DL) sampler.

Parameter	Best-fit	mean $\pm\sigma$	95% lower	95% upper
$100 w_b$	2.223	$2.223^{+0.026}_{-0.025}$	2.172	2.274
$w_{cdm}$	0.119	$0.119^{+0.0024}_{-0.0024}$	0.114	0.123
$H_0$	68.28	$68.29^{+1.0}_{-0.97}$	66.33	70.27
$\Omega_m$	0.302	$0.302^{+0.013}_{-0.014}$	0.275	0.329
$\Omega_\Lambda$	0.698	$0.698^{+0.014}_{-0.013}$	0.671	0.724

**Table 5:** Best fits values for  $\Lambda$ CDM model using Pantheon+(RNN+BNN) supernovae (DL) sampler.

Parameter	Best-fit	mean $\pm\sigma$	95% lower	95% upper
$100 w_b$	2.224	$2.226^{+0.024}_{-0.025}$	2.177	2.275
$w_{cdm}$	0.118	$0.118^{+0.002}_{-0.002}$	0.114	0.122
$M$	-19.4	$-19.4^{+0.021}_{-0.022}$	-19.44	-19.35
$H_0$	68.36	$68.47^{+0.77}_{-0.84}$	66.92	70.13
$\Omega_m$	0.301	$0.299^{+0.011}_{-0.011}$	0.2771	0.320
$\Omega_\Lambda$	0.699	$0.700^{+0.011}_{-0.011}$	0.680	0.723

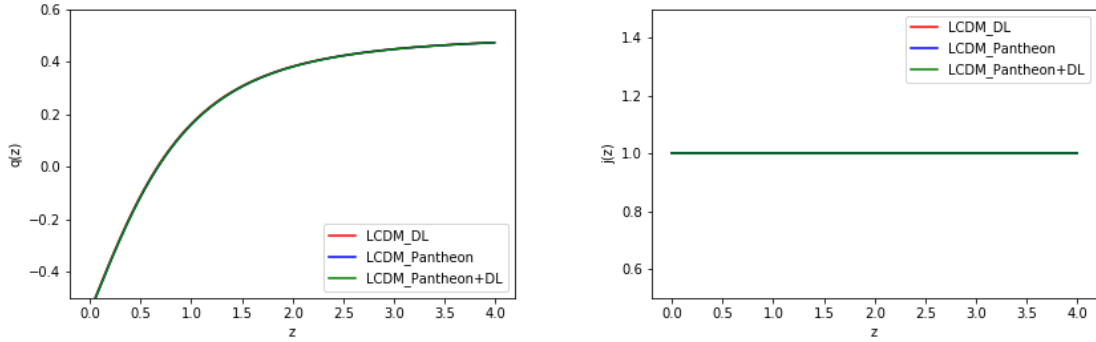


**Figure 4:** *Left:* Cosmographic parameters for  $\Lambda$ CDM. *Right:* Deceleration parameter  $q(z)$  using Pantheon observational (blue), our RNN+BNN trained supernovae sample (DL) (red) and the join of these samplers (Pantheon+DL) (green). *Left:* Jerk parameter  $j(z)$  using Pantheon observational (blue), our RNN+BNN trained supernovae sample (DL) (red) and the join of these samplers (Pantheon+DL) (green).

we should explore in detail another model. Also, this is indicated in the values of  $H_0$ ,  $\Omega_m$  and  $\Omega_\Lambda$  that seems not converge (see Tables 6-7-8). At high redshifts, both parameters recover the standard scenario.

- Case RS. We present our statistical results using Eqs. (3.10)-(3.11)-(3.12) and the steps described in (i)-(ii)-(iii) above. For this model we notice that our trained data continue overlapping the observational results in parameter spaces where there is not dependence of the cosmological parameters. We notice that when samplers are combined, the C.C are better with a correlation of the cosmological parameters at  $1-\sigma$  (see Figure 7). We compute the standard cosmographic parameter values at larger redshift (up to  $z = 4$ ) as it is shown in Figure 8 for the three samplers. Here we notice that our RNN+BNN supernovae sample does have a preference for RS in comparison to CPL model at low redshift, indicating that we should explore polynomials with  $z^2$ -factors. This is also indicated in the values of  $H_0$ ,  $\Omega_m$  and  $\Omega_\Lambda$  that seems to converge better

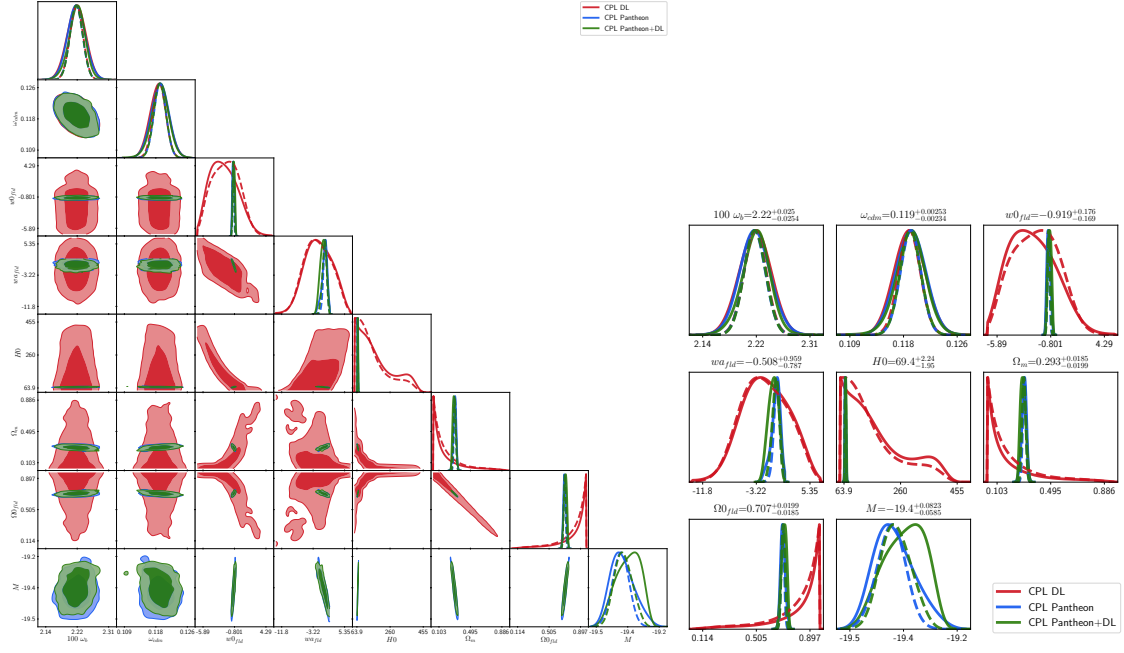


**Figure 5:** *Left:* Confidence contours, *Right:* Posterior, for CPL model using Pantheon observational (blue), our RNN+BNN trained supernovae sample (DL) (red) and the join of these samplers (Pantheon+DL) (green).

**Table 6:** Best fits values for CPL model using Pantheon sampler.

Parameter	Best-fit	mean $\pm\sigma$	95% lower	95% upper
$100 w_b$	2.219	$2.223^{+0.025}_{-0.026}$	2.172	2.275
$w_{cdm}$	0.119	$0.119^{+0.002}_{-0.002}$	0.114	0.123
$w_0$	-1.024	$-0.985^{+0.14}_{-0.17}$	-1.284	-0.641
$w_a$	0.064	$-0.158^{+0.87}_{-0.54}$	-0.698	-0.711
$M$	-19.4	$-19.39^{+0.052}_{-0.067}$	-19.52	-19.26
$H_0$	68.41	$68.64^{+1.5}_{-2}$	65.03	72.47
$\Omega_m$	0.301	$0.230^{+0.018}_{-0.015}$	0.265	0.334
$\Omega_\Lambda$	0.699	$0.700^{+0.015}_{-0.018}$	0.666	0.735

**Table 7:** Best fits values for CPL model using RNN+BNN supernovae (DL) sampler.

Parameter	Best-fit	mean $\pm\sigma$	95% lower	95% upper
$100 w_b$	2.215	$2.223^{+0.026}_{-0.026}$	2.171	2.274
$w_{cdm}$	0.117	$0.1185^{+0.002}_{-0.0024}$	0.1137	0.123
$w_0$	0.077	$-2.411^{+2.7}_{-2.1}$	-4.511	0.289
$w_a$	-0.055	$-1.749^{+4.1}_{-3.8}$	-8.729	5.576
$H_0$	64.51	$166.2^{+35}_{-1.3e+02}$	37.82	379.8
$\Omega_m$	0.335	$0.154^{+0.002}_{-0.15}$	0.004	0.156
$\Omega_\Lambda$	0.665	$0.846^{+0.15}_{-0.002}$	0.844	0.996

(see Tables 9-10-11). At high redshifts, both parameters recover the standard scenario. Interesting enough, in both CPL and RS cases, there is a deviation transition for  $j$  in  $z = [0.5, 1]$ ,



**Table 8:** Best fits values for CPL model using Pantheon+(RNN+BNN) supernovae (DL) sampler.

Parameter	Best-fit	mean $\pm\sigma$	95% lower	95% upper
100 $w_b$	2.226	2.223 $^{+0.025}_{-0.025}$	2.173	2.273
$w_{cdm}$	0.118	0.118 $^{+0.003}_{-0.002}$	0.113	0.123
$w_0$	-1.006	-0.9189 $^{+0.18}_{-0.17}$	-1.243	-0.6056
$w_a$	-0.004	-0.508 $^{+0.96}_{-0.79}$	-2.073	0.983
$M$	-19.4	-19.36 $^{+0.082}_{-0.059}$	-19.49	-19.24
$H_0$	68.58	69.43 $^{+2.2}_{-1.9}$	65.73	73.11
$\Omega_m$	0.299	0.293 $^{+0.018}_{-0.02}$	0.258	0.329
$\Omega_\Lambda$	0.701	0.707 $^{+0.02}_{-0.018}$	0.671	0.742

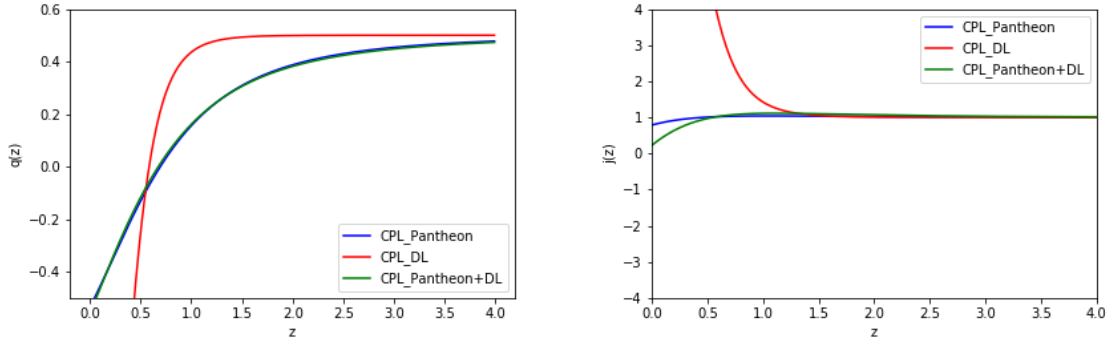


**Figure 6:** *Left:* Cosmographic parameters for CPL. *Right:* Deceleration parameter  $q(z)$  using Pantheon observational (blue), our RNN+BNN trained supernovae sample (DL) (red) and the join of these samplers (Pantheon+DL) (green). *Left:* Jerk parameter  $j(z)$  using Pantheon observational (blue), our RNN+BNN trained supernovae sample (DL) (red) and the join of these samplers (Pantheon+DL) (green).

**Table 9:** Best fits values for RS model using Pantheon sampler.

Parameter	Best-fit	mean $\pm\sigma$	95% lower	95% upper
100 $w_b$	2.224	2.222 $^{+0.026}_{-0.026}$	2.171	2.273
$w_{cdm}$	0.118	0.119 $^{+0.002}_{-0.002}$	0.114	0.123
$w_0$	-1.014	-0.986 $^{+0.16}_{-0.12}$	-1.282	-0.717
$w_a$	0.019	-0.100 $^{+0.42}_{-0.4}$	-0.918	0.726
$M$	-19.4	-19.39 $^{+0.076}_{-0.062}$	-19.54	-19.25
$H_0$	68.47	68.67 $^{+2.2}_{-2}$	64.36	72.85
$\Omega_m$	0.3	0.299 $^{+0.018}_{-0.021}$	0.260	0.340
$\Omega_\Lambda$	0.700	0.701 $^{+0.021}_{-0.018}$	0.661	0.740

redshift regions where the Padé and Chebyshev could be considered.

## 5.2 $f(z)$ CDM-like equations of state

In order to study  $H_0$  tension issues using our EoS dark energy approximants-like, we consider as a fiducial prior Late Universe measurements as:  $H_0 = 73.8 \pm 1.1 \text{ km/s/Mpc}$  from SH0ES + H0LiCOW [1] in the following models:

- Case  $f(z)$ CDM Padé-like. For this model, consider (3.17), where, as we mentioned above,  $P_0 = 1$

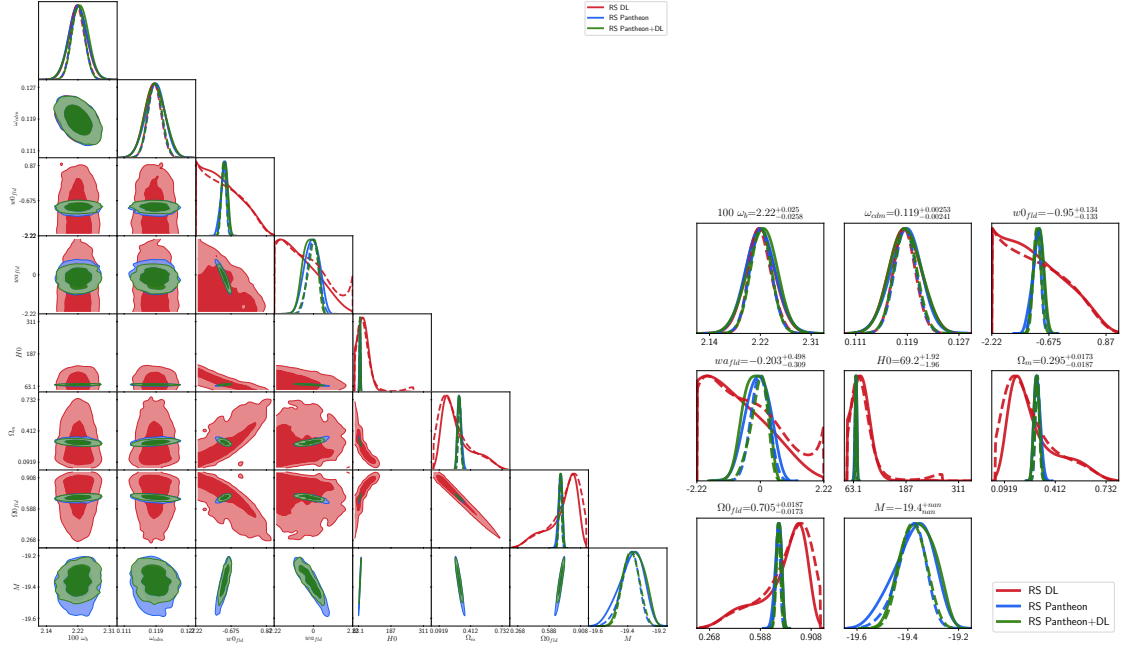


**Figure 7:** *Left:* Confidence contours, *Right:* Posterior, for RS model using Pantheon observational (blue), our RNN+BNN trained supernovae (DL) (red) and the join of these samplers (Pantheon+DL) (green).

**Table 10:** Best fits values for RS model using RNN+BNN supernovae (DL) sampler.

Parameter	Best-fit	mean $\pm\sigma$	95% lower	95% upper
$100 \omega_b$	2.22	$2.222^{+0.025}_{-0.025}$	2.172	2.272
$w_{cdm}$	0.119	$0.119^{+0.002}_{-0.003}$	0.114	0.123
$w_0$	-1.738	$-1.038^{+0.36}_{-1.2}$	-2.22	0.4432
$w_a$	1.721	$-0.7272^{+0.46}_{-1.5}$	-2.22	1.223
$H_0$	177.4	$81.61^{+16}_{-35}$	41.4	126.4
$\Omega_m$	0.045	$0.274^{+0.074}_{-0.2}$	0.045	0.611
$\Omega_\Lambda$	0.955	$0.725^{+0.2}_{-0.074}$	0.389	0.955

**Table 11:** Best fits values for RS model using Pantheon+(RNN+BNN) supernovae (DL) sampler.

Parameter	Best-fit	mean $\pm\sigma$	95% lower	95% upper
$100 \omega_b$	2.223	$2.223^{+0.025}_{-0.026}$	2.172	2.275
$\omega_{cdm}$	0.119	$0.119^{+0.003}_{-0.002}$	0.114	0.123
$w_0$	-1.014	$-0.950^{+0.13}_{-0.13}$	-1.2	-0.709
$w_a$	0.012	$-0.203^{+0.5}_{-0.31}$	-0.923	0.488
$M$	-19.4	$-19.37^{+0.001}_{-0.040}$	-19.41	-19.36
$H_0$	68.47	$69.22^{+1.900}_{-2.000}$	65.87	72.67
$\Omega_m$	0.301	$0.295^{+0.017}_{-0.019}$	0.262	0.327
$\Omega_0$	0.700	$0.705^{+0.019}_{-0.017}$	0.673	0.738

to recover Padé (2,2). To perform the numerical integration of this EoS, we consider a change of variable in terms of Padé approximants from  $z = 0$ , where  $P_0 = -P_1/Q_1$  and then integrate up to

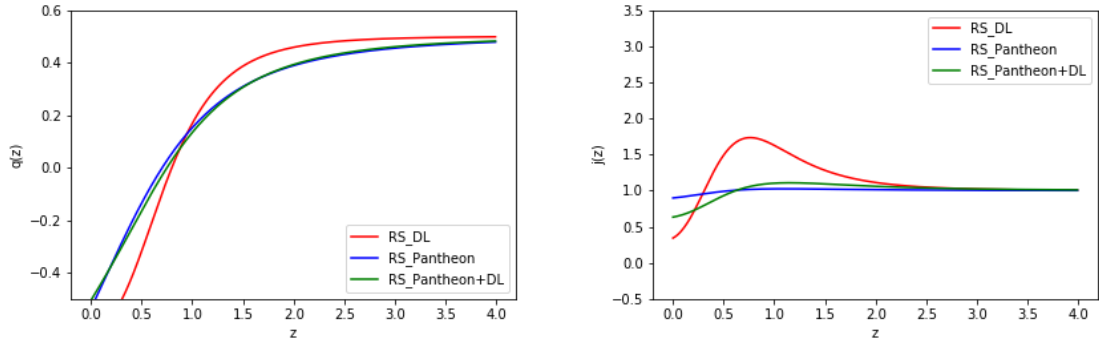


**Figure 8:** *Left:* Cosmographic parameters for RS. *Right:* Deceleration parameter  $q(z)$  using Pantheon observational (blue), our RNN+BNN trained supernovae sample (DL) (red) and the join of these samplers (Pantheon+DL) (green). *Left:* Jerk parameter  $j(z)$  using Pantheon observational (blue), our RNN+BNN trained supernovae sample (DL) (red) and the join of these samplers (Pantheon+DL) (green).

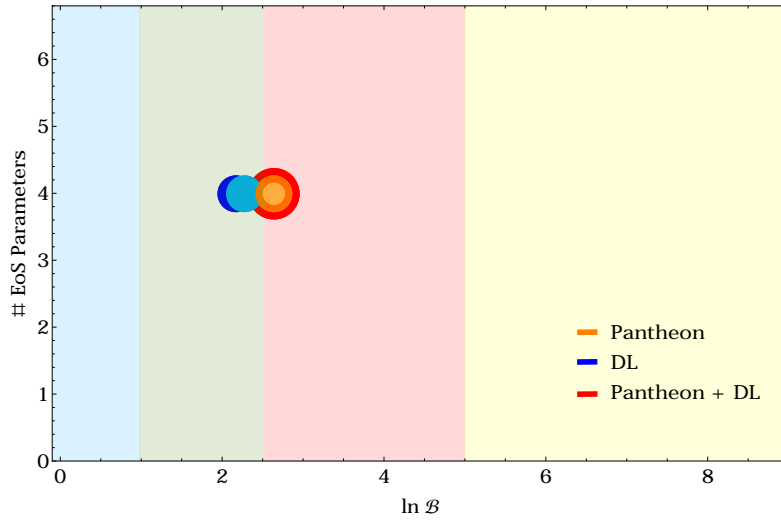


**Figure 9:** Bayesian portrait for CPL and RS according to the number of free EoS parameters using the values given in Tables 6-7-8 and 9-10-11. The qualitative color regions represent Jeffrey's scale as: strong evidence in favour of hypothesis model (light-yellow), moderate evidence in favour of hypothesis model (light-red), weak evidence for hypothesis model (light-green) and inconclusive evidence (light-blue). Each color in the plot legend indicates the sampler used to calculate the value  $\ln B_{ij}$  in comparison to  $\Lambda$ CDM model. For each sampler, the light color circles denote the RS model and the darker color circles denote the CPL model. This option was selected since the models overlap statistically for the observational sampler and the join sampler.

$P_0 = 1$ . In this manner we avoid any possible divergency due the Padé approximant. We notice a high correlation between the approximants of the model and the cosmological parameters for our three samplers, see Figure 10 and Tables 12-13-14. The analyses with Pantheon and DL show positive bestfits values for the approximants  $P_1$  and  $P_2$ , which is in agreement with the theoretical analysis from Figure 1. For the approximants  $Q_1$  and  $Q_2$  with contrary values in each sampler cases, this is a remanent of the transition from a deceleration phase to an acceleration one as we can see from Figure 11. We observe also that the cosmographic parameters  $q$  and  $j$  are indistinguishable between each other for Pantheon+DL and Pantheon samplers.

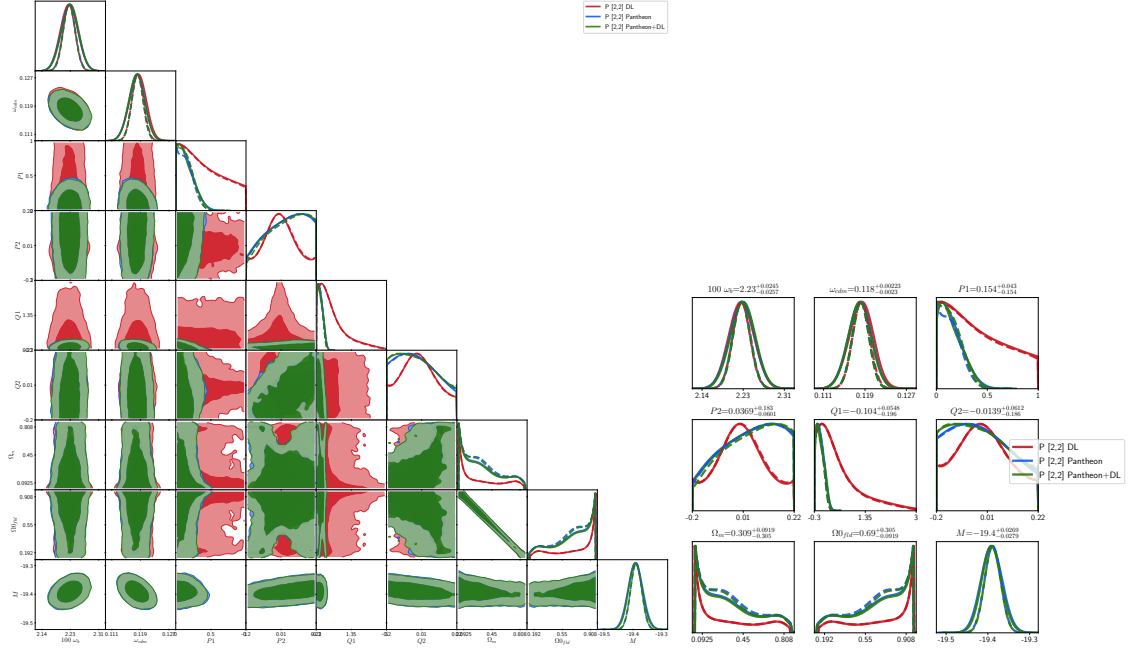


**Figure 10:** *Left:* Confidence contours, *Right:* Posterior, for  $f(z)$ CDM Padé-like model using Pantheon observational (blue), our RNN+BNN trained supernovae sample (DL) (red) and the join of these samplers (Pantheon+DL) (green).

**Table 12:** Best fits values for  $f(z)$ CDM Padé-like model using Pantheon sampler.

Parameters	Best-fit	mean $\pm\sigma$	95% lower	95% upper
$100 w_b$	2.222	$2.225^{+0.026}_{-0.025}$	2.174	2.275
$w_{cdm}$	0.118	$0.118^{+0.002}_{-0.002}$	0.114	0.123
$P_1$	0.183	$0.156^{+0.043}_{-0.16}$	$1.462e - 06$	0.376
$P_2$	0.040	$0.035^{+0.18}_{-0.061}$	-0.162	0.22
$Q_1$	-0.204	$-0.107^{+0.053}_{-0.19}$	-0.3	0.131
$Q_2$	0.0262	$-0.013^{+0.06}_{-0.19}$	-0.2	0.186
$M$	-19.4	$-19.4^{+0.028}_{-0.029}$	-19.46	-19.34
$\Omega_m$	0.251	$0.311^{+0.093}_{-0.31}$	0.001	0.404
$\Omega_0$	0.749	$0.688^{+0.31}_{-0.093}$	0.595	0.998

**Table 13:** Best fits values for  $f(z)$ CDM Padé-like using RNN+BNN supernovae (DL) sampler.

Parameter	Best-fit	mean $\pm\sigma$	95% lower	95% upper
$100 w_b$	2.223	$2.224^{+0.025}_{-0.025}$	2.173	2.274
$w_{cdm}$	0.118	$0.118^{+0.002}_{-0.002}$	0.114	0.123
$P_1$	0.089	$0.411^{+0.14}_{-0.41}$	$7.315e - 06$	0.921
$P_2$	0.151	$0.004^{+0.099}_{-0.11}$	-0.188	0.196
$Q_1$	-0.222	$0.506^{+0.14}_{-0.81}$	-0.3	2.07
$Q_2$	-0.137	$-0.004^{+0.094}_{-0.14}$	-0.2	0.183
$\Omega_m$	0.0142	$0.28^{+0.002}_{-0.001}$	0.281	0.282
$\Omega_0$	0.986	$0.720^{+0.002}_{-0.001}$	0.721	0.722

**Table 14:** Best fits values for  $f(z)$ CDM Padé-like model using Pantheon+(RNN+BNN) supernovae (DL) sampler.

Parameter	Best-fit	mean $\pm\sigma$	95% lower	95% upper
$100 w_b$	2.221	$2.226^{+0.025}_{-0.026}$	2.176	2.276
$w_{cdm}$	0.119	$0.118^{+0.002}_{-0.002}$	0.114	0.123
$P_1$	0.108	$0.154^{+0.043}_{-0.15}$	$1.897e-05$	0.366
$P_2$	-0.007	$0.0370^{+0.18}_{-0.06}$	-0.161	0.22
$Q_1$	-0.163	$-0.104^{+0.055}_{-0.2}$	-0.3	0.135
$Q_2$	0.055	$-0.013^{+0.061}_{-0.19}$	-0.203	0.048
$M$	-19.4	$-19.4^{+0.027}_{-0.028}$	-19.45	-19.34
$\Omega_m$	0.424	$0.310^{+0.092}_{-0.3}$	0.01	0.402
$\Omega_0$	0.575	$0.690^{+0.3}_{-0.092}$	0.600	0.990

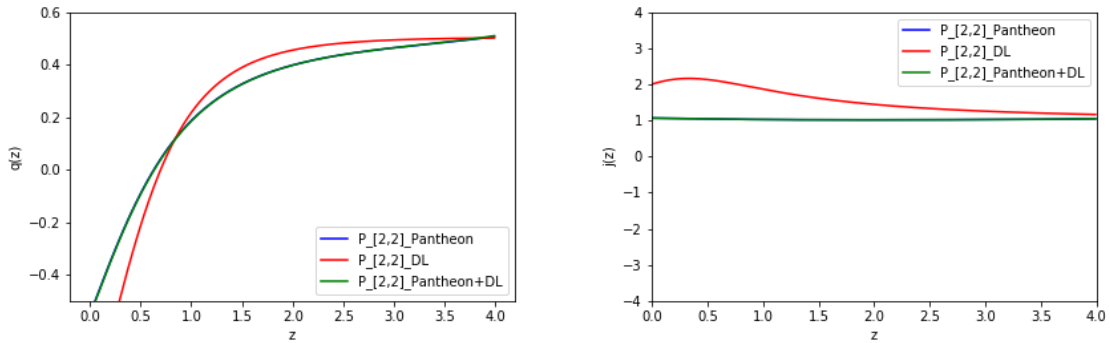


**Figure 11:** *Left:* Cosmographic parameters for  $f(z)$ CDM Padé. *Right:* Deceleration parameter  $q(z)$  using Pantheon observational (blue), our RNN+BNN trained supernovae sample (DL) (red) and the join of these samplers (Pantheon+DL) (green). *Left:* Jerk parameter  $j(z)$  using Pantheon observational (blue), our RNN+BNN trained supernovae sample (DL) (red) and the join of these samplers (Pantheon+DL) (green).

- Case  $f(z)$ CDM Chebyshev-like. As in the latter, for this model, consider (3.23), where  $a_3 = a_1/b_1$  to recover Chebyshev (2,1). To perform the numerical integration of the EoS, we consider now a change of variable in terms of Chebyshev approximants from  $a_0 = 0$  up to  $a_2 = -a_1/b_1$ . In this manner we avoid any possible divergency and recover the original Chebyshev approximant. The results for this case are reported in Tables 15-16-17 and Figure 12. For this kind of polynomial  $R_{(2,1)}$  we found a high correlation between approximants, but the confidence regions for the DL simulations gets to reproduce the same observational trend at 95%. The analyses with Pantheon and DL show a couple of positive bestfits values for the approximants  $a_1$  and  $a_2$  and negative values for  $b_1$ , in agreement with the theoretical analysis from Figure 1. From Figure 13 we notice deviations from  $q$  and  $j$  in comparison to the observational and join sampler, but at high redshift the three tested samplers for this model are asymptotically approaching.

## 6 Discussion

In this work we presented a proposal that consists in an *inverse cosmography* from where we can compute a *generic* EoS without assuming directly a cosmographic series. In this approach is possible to relax a couple of cosmography problems, as e.g truncation issues over the series/polynomials proposed. Also, we developed the study of the dark energy dynamics, without a  $\Lambda$ , by proposing suitable Padé or

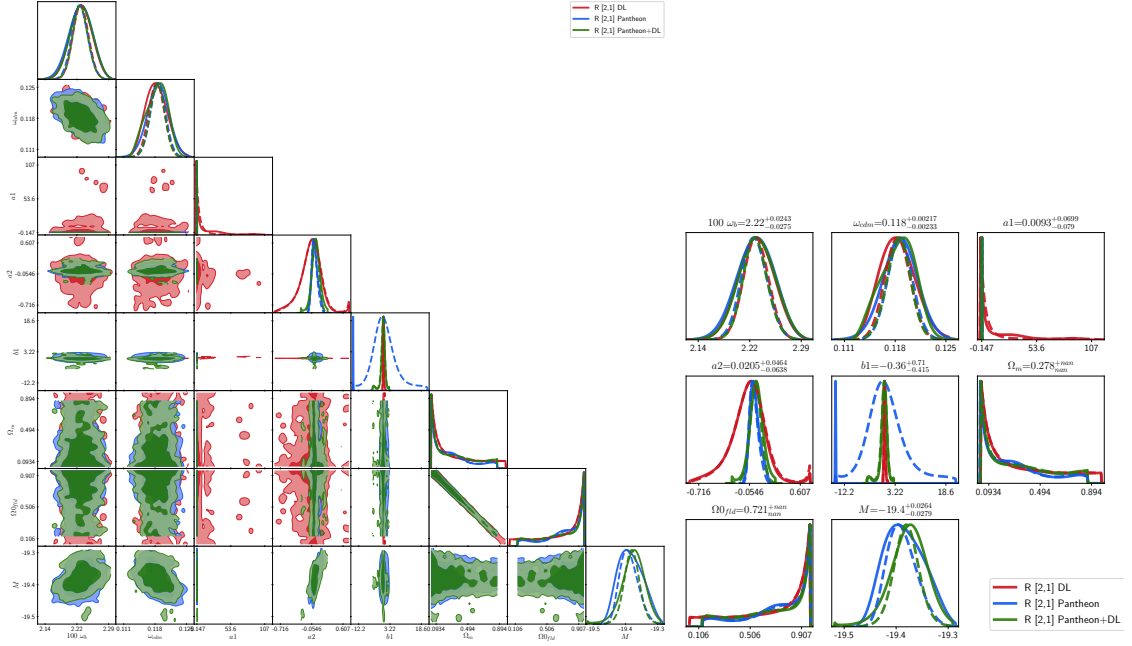


**Figure 12:** *Left:* Confidence contours, *Right:* Posterior, for  $f(z)$ CDM Chebyshev-like model using Pantheon observational (blue), our RNN+BNN trained supernovae sample (DL) (red) and the join of these samplers (Pantheon+DL) (green).

**Table 15:** Best fits values for  $f(z)$ CDM Chebyshev-like model using Pantheon sampler.

Parameter	Best-fit	mean $\pm\sigma$	95% lower	95% upper
$100 w_b$	2.222	$2.223^{+0.028}_{-0.026}$	2.168	2.277
$w_{cdm}$	0.119	$0.119^{+0.002}_{-0.002}$	0.114	0.123
$a_1$	0.026	$0.013^{+0.055}_{-0.065}$	-0.102	0.134
$a_2$	-0.009	$0.016^{+0.001}_{-0.002}$	0.014	0.017
$b_1$	0.587	$0.140^{+1.1}_{-0.73}$	-1.632	2.252
$M$	-19.4	$-19.39^{+0.001}_{-0.005}$	-19.39	-19.39
$\Omega_m$	0.134	$0.248^{+0.001}_{-0.005}$	0.243	0.245
$\Omega_0$	0.866	$0.752^{+0.001}_{-0.005}$	0.745	0.753

**Table 16:** Best fits values for  $f(z)$ CDM Chebyshev-like using RNN+BNN supernovae (DL) sampler.

Parameter	Best-fit	mean $\pm\sigma$	95% lower	95% upper
$100 w_b$	2.22	$2.225^{+0.027}_{-0.024}$	2.175	2.278
$w_{cdm}$	0.119	$0.118^{+0.002}_{-0.003}$	0.114	0.123
$a_1$	-0.616	$3.796^{+2.8}_{-8.2}$	-4.404	6.596
$a_2$	0.599	$-0.059^{+0.21}_{-0.13}$	-0.188	0.152
$b_1$	-0.027	$0.038^{+0.14}_{-0.2}$	-0.162	0.178
$\Omega_m$	0.256	$0.291^{+0.001}_{-0.002}$	0.289	0.292
$\Omega_0$	0.744	$0.708^{+0.001}_{-0.002}$	0.706	0.709

Chebyshev polynomials evolving with a cold dark matter (CDM) fluid. All these models were tested with current supernovae data and deep learning for supernovae trained sampler. This machine learning

**Table 17:** Best fits values for  $f(z)$ CDM Chebyshev-like model using Pantheon+(RNN+BNN) super-novae (DL) sampler.

Parameter	Best-fit	mean $\pm\sigma$	95% lower	95% upper
$100 w_b$	2.225	$2.225^{+0.024}_{-0.028}$	2.175	2.279
$w_{cdm}$	0.119	$0.118^{+0.002}_{-0.002}$	0.114	0.123
$a_1$	0.017	$0.009^{+0.07}_{-0.079}$	-0.149	0.162
$a_2$	0.001	$0.021^{+0.046}_{-0.064}$	-0.119	0.251
$b_1$	-1.618	$-0.360^{+0.71}_{-0.41}$	-0.77	0.350
$M$	-19.4	$-19.39^{+0.026}_{-0.028}$	-19.44	-19.32
$\Omega_m$	0.262	$0.278^{+0.001}_{-0.001}$	0.277	0.279
$\Omega_0$	0.738	$0.722^{+0.001}_{-0.001}$	0.720	0.722

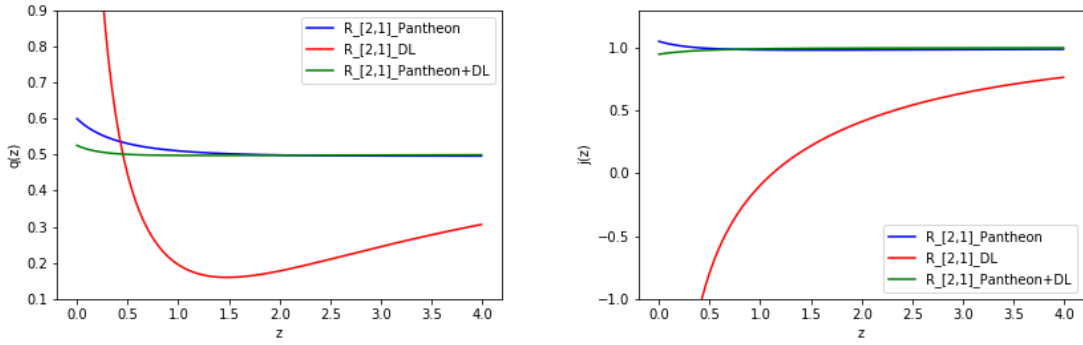


**Figure 13:** *Left:* Cosmographic parameters for  $f(z)$ CDM Chebyshev. *Right:* Deceleration parameter  $q(z)$  using Pantheon observational (blue), our RNN+BNN trained supernovae sample (DL) (red) and the join of these samplers (Pantheon+DL) (green). *Left:* Jerk parameter  $j(z)$  using Pantheon observational (blue), our RNN+BNN trained supernovae sample (DL) (red) and the join of these samplers (Pantheon+DL) (green).

Model	$\chi^2$	$q_0$	$j_0$	$\ln B_{ij}$	AIC	BIC
$\Lambda$ CDM	1028	$-0.551 \pm 0.014$	1.0	-	-	-
CPL	1028	$-0.534 \pm 0.308$	$0.790 \pm 1.011$	2.637	1036	1055.4
RS	1028	$-0.536 \pm 0.335$	$0.9 \pm 1.312$	2.637	1036	1055.4
$f(z)$ CDM Padé-like	1028	$-0.550 \pm 0.354$	$1.063 \pm 0.282$	2.637	1036	1055.94
$f(z)$ CDM Chebyshev-like	1028	$0.599 \pm 0.184$	$1.050 \pm 0.460$	3.042	1038	1062.92

**Table 18:** Cosmological models and approximants using Pantheon sampler. Column 1: cosmographic parameters values at  $2\text{-}\sigma$ . Column 2: Bayes factor. Column 3 and 4: information criteria AIC and BIC, respectively.

architecture can train a homogeneous SNeIa sampler in where the resulting dynamics of dark energy could lead to the necessity of another cosmological model different from  $\Lambda$ CDM. In this panorama, our inverse cosmography approach can fit very well since is not necessary to consider higher-order corrections of the cosmography series to obtain a convergence best fit in comparison to the standard dark energy EoSs as our Bayesian analyses show (see Tables 18-19-20). The advantage to joint current and trained supernovae sampler is the density information data that we acquire in a redshift range of  $0.01 < z < 4$ , which is larger than the observable one. From the results of the Bayesian evidence we notice that models polynomial-like, as Padé and Chebyshev lies in better significant regions in



Model	$\chi^2$	$q_0$	$j_0$	$\ln B_{ij}$	AIC	BIC
$\Lambda$ CDM	7.991	$-0.550 \pm 0.020$	1.0	-	-	-
CPL	2.75	$-1.721 \pm 6.564$	$11.716 \pm 66.16$	2.163	10.72	30.659
RS	3.81	$-0.632 \pm 0.8272$	$0.344 \pm 2.7626$	2.281	11.81	31.749
$f(z)$ CDM Padé-like	7.97	$-0.910 \pm 0.142$	$2.00 \pm 0.601$	7.594	15.97	35.909
$f(z)$ CDM Chebyshev-like	7.96	$4.358 \pm 5.989$	$-7.643 \pm 12.606$	7.588	17.96	42.884

**Table 19:** Cosmological models and approximants using trained DL Pantheon sampler. Column 1: cosmographic parameters values at  $2\text{-}\sigma$ . Column 2: Bayes factor. Column 3 and 4: information criteria AIC and BIC, respectively.

Model	$\chi^2$	$q_0$	$j_0$	$\ln B_{ij}$	AIC	BIC
$\Lambda$ CDM	1035	$-0.551 \pm 0.016$	1.0	-	-	-
CPL	1035	$-0.475 \pm 0.380$	$0.224 \pm 2.240$	2.637	1062.94	1043
RS	1035	$-0.505 \pm 0.286$	$0.634 \pm 1.309$	2.637	1062.94	1043
$f(z)$ CDM Padé-like	1035	$-0.552 \pm 0.35$	$1.070 \pm 0.281$	2.637	1043	1062.94
$f(z)$ CDM Chebyshev-like	1035	$0.525 \pm 0.445$	$0.947 \pm 0.605$	3.042	1045	1069.92

**Table 20:** Cosmological models and approximants using Pantheon + DL Pantheon samplers. Column 1: cosmographic parameters values at  $2\text{-}\sigma$ . Column 2: Bayes factor. Column 3 and 4: information criteria AIC and BIC, respectively.

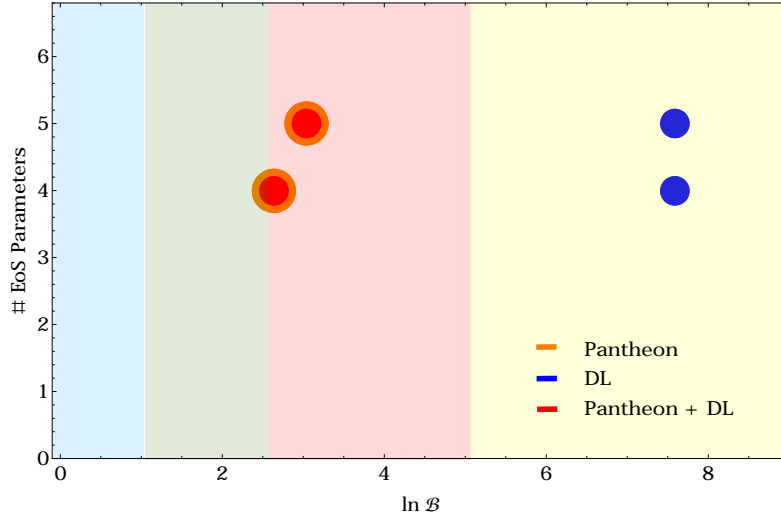


**Figure 14:** Bayesian portrait for Padé (2,2) and Chebyshev (2,1) according to the number of free EoS parameters using the values given in Tables 12-13-14 and 15-16-17. The qualitative color regions represent Jeffrey's scale as: strong evidence in favour of hypothesis model (light-yellow), moderate evidence in favour of hypothesis model (light-red), weak evidence for hypothesis model (light-green) and inconclusive evidence (light-blue). Each color in the plot legend indicates the sampler used to calculate the value  $\ln B_{ij}$  in comparison to  $\Lambda$ CDM model. For each sampler, the light color circles denote the Padé model and the darker color circles denote the Chebyshev model. This option was selected since the models overlap statistically for the observational sampler and the join sampler.

comparison to the standard ones (see Figure 9). Furthermore,  $f(z)$ CDM Padé-like and  $f(z)$ CDM Chebyshev-like are decisive in comparison to  $\Lambda$ CDM using DL sampler (see Figure 14).

Now, from the perspective of the EoS's (see Figure 15), we obtained the following results: in the case  $f(z)$ CDM Padé-like we obtain a dynamical EoS with a transition from  $\Lambda$ CDM to a quintessence

scenario. A deviation of  $1\text{-}\sigma$  from the standard model can be observed using Pantheon and join sampler. For this case we notice that  $f(z)$ CDM Padé-like model does not have any divergence in the observational redshift range as it was reported in the mentioned references. Also, this model mimics  $\Lambda$ CDM at low redshift. On the contrary,  $f(z)$ CDM Chebyshev-like model does present a divergency at low redshift, but at high redshift starts to mimic  $f(z)$ CDM Padé-like model. Notice how all the tested models reproduce the theoretical scenarios reported in Figure 1.

Interestingly enough, so far until our knowledge, there is not available a CLASS + MontePython code adapted for cosmography, which results quite tricky since we need to introduce directly the definition of the modulus distance and then deal with series divergencies. Meanwhile, using inverse cosmography it is possible to adapt easily the numerical codes and obtain a theoretical convergence<sup>9</sup>. The inclusion of observable data from another nature that can give us information at higher redshifted universe will enrich the convergence of a series with more exotic polynomials. This future study will be reported elsewhere.

## Acknowledgments

CE-R acknowledges the *Royal Astronomical Society* as FRAS 10147. The authors are supported by *PAPIIT* Project IA100220 and ICN-UNAM projects. This article is also based upon work from COST action CA18108, supported by COST (European Cooperation in Science and Technology). The Authors also thanks M. Carvajal, H. Quevedo and O. Luongo for their useful discussions.

## A Generic cosmographic parameters

In this Appendix we present the exact solutions of the cosmographic parameters for the models treated and in term of the cosmological parameters.

### A.1 Chevallier-Polarski-Linder (CPL) case

With the inverse cosmography prescription (2.7)-(2.8)-(2.9), we can obtain the following cosmographic parameters for this model as follow:

$$q(z) = \frac{(\Omega_m - 1)(z + 1)^{3(w_a + w_0)}(3zw_a + 3w_0(z + 1) + z + 1) - (z + 1)\Omega_m e^{\frac{3zw_a}{z+1}}}{2(\Omega_m - 1)(z + 1)^{3w_a + 3w_0 + 1} - 2(z + 1)\Omega_m e^{\frac{3zw_a}{z+1}}}, \quad (\text{A.1})$$

$$\begin{aligned} j(z) = & \frac{(\Omega_m - 1)(9z^2w_a^2 + 3(3z + 1)(z + 1)w_a + 2(z + 1)^2)(z + 1)^{3(w_a + w_0)}}{2(z + 1)^2 \left( (\Omega_m - 1)(z + 1)^{3(w_a + w_0)} - \Omega_m e^{\frac{3zw_a}{z+1}} \right)} \\ & + \frac{9w_0(\Omega_m - 1)(2zw_a + z + 1)(z + 1)^{3w_a + 3w_0 + 1}}{2(z + 1)^2 \left( (\Omega_m - 1)(z + 1)^{3(w_a + w_0)} - \Omega_m e^{\frac{3zw_a}{z+1}} \right)} \\ & + \frac{9w_0^2(\Omega_m - 1)(z + 1)^{3w_a + 3w_0 + 2} - 2(z + 1)^2\Omega_m e^{\frac{3zw_a}{z+1}}}{2(z + 1)^2 \left( (\Omega_m - 1)(z + 1)^{3(w_a + w_0)} - \Omega_m e^{\frac{3zw_a}{z+1}} \right)}, \end{aligned} \quad (\text{A.2})$$

$$\begin{aligned} s(z) = & \left[ \frac{(\Omega_m - 1)(z + 1)^{3(w_a + w_0)}}{2(\Omega_m - 1)(z + 1)^{3w_a + 3w_0 + 4} - 2(z + 1)^4\Omega_m e^{\frac{3zw_a}{z+1}}} \right] \\ & \times (-9z^3w_a^3 + (z + 1)^2w_a(-9w_0(3w_0z - 2(z - 1)z + 1) + 9z^2 + z - 2) \\ & + 9z(z + 1)w_a^2(-3w_0z + (z - 1)z - 1) \\ & + (9w_0(w_0 + 1) + 2)(z + 1)^3(z - w_0)) - 2z(z + 1)^3\Omega_m e^{\frac{3zw_a}{z+1}}, \end{aligned} \quad (\text{A.3})$$

<sup>9</sup>The code will be released after publication.

## A.2 Redshift squared (RS) case

With the inverse cosmography prescription (2.7)-(2.8)-(2.9), we can obtain the following cosmographic parameters for this model as follow:

$$\frac{2}{3}(q(z) + 1) = \frac{\left( \Omega_m - (\Omega_m - 1)(z + 1)^{3w_0} (z^2 + 1)^{\frac{3w_a}{2} - 1} (z(z + 1)w_a + (w_0 + 1)(z^2 + 1)) \right)}{\Omega_m - (\Omega_m - 1)(z + 1)^{3w_0} (z^2 + 1)^{\frac{3w_a}{2}}}, \quad (\text{A.4})$$

$$2j(z) = \frac{3(\Omega_m - 1)(z + 1)^{3w_0}}{(z^2 + 1)^2 \left( (\Omega_m - 1)(z + 1)^{3w_0} - \Omega_m (z^2 + 1)^{-\frac{3w_a}{2}} \right)} \times ((z + 1)w_a (6w_0 (z^3 + z) + z(z(3z - 1) + 5) + 1) + 3z^2(z + 1)^2 w_a^2 + 3w_0 (w_0 + 1)(z^2 + 1)^2) + 2, \quad (\text{A.5})$$

$$s(z) = \frac{3(\Omega_m - 1)(z + 1)^{3w_0}}{6(z + 1)(z^2 + 1)^3 \left( (\Omega_m - 1)(z + 1)^{3w_0} (z^2 + 1)^{\frac{3w_a}{2}} - \Omega_m \right)} \times (z^2 + 1)^{\frac{3w_a}{2}} (-9z^3(z + 1)^3 w_a^3 + 9z(z + 1)^2 w_a^2 (-3w_0 (z^3 + z) + z(z((z - 1)z + 2) - 3) - 1) + (z + 1)w_a(9w_0(z^2 + 1) \times (-3w_0(z^3 + z) + z(z(2(z - 1)z + 3) - 4) - 1) + z(z(z(z(9z - 5) + 26) - 8) + 27) - 3) - 6) + (9w_0(w_0 + 1) + 2)(z^2 + 1)^3 (z - w_0)) - 6z(z^2 + 1)^3 \Omega_m. \quad (\text{A.6})$$

## A.3 $f(z)$ CDM Padé-like case

With the inverse cosmography prescription (2.7)-(2.8)-(2.9), we can obtain the following cosmographic parameters for this model as follow:

$$q(z) = \frac{(z + 1) \left( 3(z + 1)^2 \Omega_m + \frac{\Omega_p(P_1(Q_2 z^2 - 1) + P_2 z(Q_1 z + 2) - 2Q_2 z - Q_1)}{(z(Q_2 z + Q_1) + 1)^2} \right)}{2 \left( (z + 1)^3 \Omega_m + \frac{\Omega_p(P_2 z^2 - P_1 z + 1)}{z(Q_2 z + Q_1) + 1} \right)} - 1, \quad (\text{A.7})$$

$$\frac{j(z)}{(z + 1)\Omega_p} - 1 = \frac{P_1(Q_2^2(-(2z + 1))z^3 + Q_1(-Q_2 z^3 + 2z + 1) + 3Q_2(z + 1)z + 1)}{(z(Q_2 z + Q_1) + 1)^2 ((z + 1)^3 \Omega_m (z(Q_2 z + Q_1) + 1) + \Omega_p(P_2 z^2 - P_1 z + 1))} + \frac{P_2(z^2(-Q_1(Q_1 z + 3) - Q_2(Q_1(2z + 1)z + 5z + 3)) - z + 1)}{(z(Q_2 z + Q_1) + 1)^2 ((z + 1)^3 \Omega_m (z(Q_2 z + Q_1) + 1) + \Omega_p(P_2 z^2 - P_1 z + 1))} + \frac{Q_2^2 z^2(5z + 3) + Q_2(3Q_1(2z + 1)z + z - 1) + Q_1(2Q_1 z + Q_1 + 1)}{(z(Q_2 z + Q_1) + 1)^2 ((z + 1)^3 \Omega_m (z(Q_2 z + Q_1) + 1) + \Omega_p(P_2 z^2 - P_1 z + 1))}, \quad (\text{A.8})$$

$$\begin{aligned}
\frac{1-s(z)}{(z+1)} = & \frac{(z+1)\Omega_m(z(Q_2z+Q_1)+1)^4}{(z(Q_2z+Q_1)+1)^3((z+1)^3\Omega_m(z(Q_2z+Q_1)+1)+\Omega_p(P_2z^2-P_1z+1))} \\
& + \frac{\Omega_p(Q_2^3z^3(P_1z(2z(z+1)+1)-z(5z+7)-4))}{(z(Q_2z+Q_1)+1)^3((z+1)^3\Omega_m(z(Q_2z+Q_1)+1)+\Omega_p(P_2z^2-P_1z+1))} \\
& + \frac{Q_2^2z(P_1z(Q_1(3z+1)z^2-(z+8)z-6)-Q_1(z(11z+12)+6)z-6z^2+2z+4)}{(z(Q_2z+Q_1)+1)^3((z+1)^3\Omega_m(z(Q_2z+Q_1)+1)+\Omega_p(P_2z^2-P_1z+1))} \\
& + \frac{Q_2(P_1(Q_1^2z^4-4Q_1(z+1)^2z-2(2z+1)z+1))}{(z(Q_2z+Q_1)+1)^3((z+1)^3\Omega_m(z(Q_2z+Q_1)+1)+\Omega_p(P_2z^2-P_1z+1))} \\
& + \frac{2Q_1(-2Q_1(2z(z+1)+1)z-4z^2+1)-z+P_2(Q_2^2z^3(Q_1z(2z(z+1)+1))}{(z(Q_2z+Q_1)+1)^3((z+1)^3\Omega_m(z(Q_2z+Q_1)+1)+\Omega_p(P_2z^2-P_1z+1))} \\
& + \frac{z(5z+7)+4+Q_2z(Q_1z^2(Q_1(3z+1)z+10z+4)+2(z-1)(3z+2))}{(z(Q_2z+Q_1)+1)^3((z+1)^3\Omega_m(z(Q_2z+Q_1)+1)+\Omega_p(P_2z^2-P_1z+1))} \\
& + \frac{Q_1(Q_1z^3(Q_1z+4)+4z^2-2z-1)+z}{(z(Q_2z+Q_1)+1)^3((z+1)^3\Omega_m(z(Q_2z+Q_1)+1)+\Omega_p(P_2z^2-P_1z+1))} \\
& + \frac{Q_1(-(P_1+Q_1)(Q_1(2z(z+1)+1)+3z)-Q_1)}{(z(Q_2z+Q_1)+1)^3((z+1)^3\Omega_m(z(Q_2z+Q_1)+1)+\Omega_p(P_2z^2-P_1z+1))} \\
& - \frac{(P_1+1)Q_1+Q_2-(P_1+P_2)\Omega_p}{(z(Q_2z+Q_1)+1)^3((z+1)^3\Omega_m(z(Q_2z+Q_1)+1)+\Omega_p(P_2z^2-P_1z+1))}, \tag{A.9}
\end{aligned}$$

#### A.4 $f(z)$ CDM Chebyshev-like case

With the inverse cosmography prescription (2.7)-(2.8)-(2.9), we can obtain the following cosmographic parameters for this model as follow:

$$q(z) = \frac{(z+1)(\Omega_p(2a_2z(b_1z+2)-a_3b_1+a_1)+3(z+1)^2(b_1z+1)^2\Omega_m)}{2(b_1z+1)((z(2a_2z+a_1)+a_3)\Omega_p+(z+1)^3(b_1z+1)\Omega_m)} - 1, \tag{A.10}$$

$$\begin{aligned}
j(z) = & \frac{\Omega_p(a_1(b_1(b_1z^3-3z-1)-1)+b_1(a_3(b_1(3z(z+1)+1)+3z+1))}{(b_1z+1)^2((z(2a_2z+a_1)+a_3)\Omega_p+(z+1)^3(b_1z+1)\Omega_m)} \\
& - \frac{2a_2z^2(b_1z+z+3)+2a_2+a_3+(z+1)^3(b_1z+1)^3\Omega_m}{(b_1z+1)^2((z(2a_2z+a_1)+a_3)\Omega_p+(z+1)^3(b_1z+1)\Omega_m)}, \tag{A.11}
\end{aligned}$$

$$\begin{aligned}
s(z) = & \frac{\Omega_p(a_1(b_1(b_1z^3-3z-1)-1)+b_1(a_3(b_1(3z(z+1)+1)+3z+1))}{(b_1z+1)^2((z(2a_2z+a_1)+a_3)\Omega_p+(z+1)^3(b_1z+1)\Omega_m)} \\
& - \frac{2a_2z^2(b_1z+z+3)+2a_2+a_3+(z+1)^3(b_1z+1)^3\Omega_m}{(b_1z+1)^2((z(2a_2z+a_1)+a_3)\Omega_p+(z+1)^3(b_1z+1)\Omega_m)}. \tag{A.12}
\end{aligned}$$

## References

- [1] L. Verde, T. Treu and A. G. Riess, Nature Astronomy 2019 doi:10.1038/s41550-019-0902-0 [arXiv:1907.10625 [astro-ph.CO]].
- [2] Y. L. Bolotin, V. A. Cherkaskiy, O. Y. Ivashtenko, M. I. Konchatnyi and L. G. Zazunov, arXiv:1812.02394 [gr-qc].
- [3] S. Capozziello, M. De Laurentis, O. Luongo and A. Ruggeri, Galaxies **1**, 216 (2013) doi:10.3390/galaxies1030216 [arXiv:1312.1825 [gr-qc]].
- [4] C. Escamilla-Rivera and S. Capozziello, Int. J. Mod. Phys. D **28**, no. 12, 1950154 (2019) doi:10.1142/S0218271819501542 [arXiv:1905.04602 [gr-qc]].
- [5] C. Escamilla-Rivera, M. A. C. Quintero and S. Capozziello, JCAP **03** (2020) no.03, 008 doi:10.1088/1475-7516/2020/03/008 [arXiv:1910.02788 [astro-ph.CO]].

- [6] S. Capozziello, R. D’Agostino and O. Luongo, Int. J. Mod. Phys. D **28**, no. 10, 1930016 (2019) doi:10.1142/S0218271819300167 [arXiv:1904.01427 [gr-qc]].
- [7] <https://www.desi.lbl.gov> <https://www.lsst.org>
- [8] D. J. Schlegel *et al.*, arXiv:1907.11171 [astro-ph.IM].
- [9] Bowman, J., Rogers, A., Monsalve, R. et al. Nature 555, 67–70 (2018).
- [10] M. Corman, C. Escamilla-Rivera and M. Hendry, [arXiv:2004.04009 [astro-ph.CO]].
- [11] [LIGO Scientific and Virgo], [arXiv:2004.08342 [astro-ph.HE]].
- [12] C. Escamilla-Rivera and J. C. Fabris, Galaxies **4**, no. 4, 76 (2016) doi:10.3390/galaxies4040076 [arXiv:1511.07066 [astro-ph.CO]].
- [13] E. K. Li, M. Du and L. Xu, Mon. Not. Roy. Astron. Soc. **491**, no. 4, 4960 (2020) doi:10.1093/mnras/stz3308
- [14] C. Gruber and O. Luongo, Phys. Rev. D **89**, no. 10, 103506 (2014) doi:10.1103/PhysRevD.89.103506
- [15] S. Capozziello, R. D’Agostino and O. Luongo, Mon. Not. Roy. Astron. Soc. **476**, no. 3, 3924 (2018) doi:10.1093/mnras/sty422 [arXiv:1712.04380 [astro-ph.CO]].
- [16] A. Aviles, C. Gruber, O. Luongo and H. Quevedo, Phys. Rev. D **86**, 123516 (2012) doi:10.1103/PhysRevD.86.123516 [arXiv:1204.2007 [astro-ph.CO]].
- [17] M. Benetti and S. Capozziello, JCAP **1912**, no. 12, 008 (2019) doi:10.1088/1475-7516/2019/12/008 [arXiv:1910.09975 [astro-ph.CO]].
- [18] C. Escamilla-Rivera, Galaxies **4** (2016) 8.
- [19] M. Chevallier, D. Polarski, Int. J. Mod. Phys. D **10** (2001) 213.
- [20] E.V. Linder, Gen. Rel. Grav. **40** (2008) 329.
- [21] E.M. Jr. Barboza, J.S. Alcaniz, Phys. Lett. B **666** (2008) 415.
- [22] A. Aviles, J. Klapp and O. Luongo, Phys. Dark Univ. **17**, 25 (2017) doi:10.1016/j.dark.2017.07.002 [arXiv:1606.09195 [astro-ph.CO]].
- [23] S. Capozziello, Ruchika and A. A. Sen, Mon. Not. Roy. Astron. Soc. **484**, 4484 (2019) doi:10.1093/mnras/stz176 [arXiv:1806.03943 [astro-ph.CO]].
- [24] A. R. Liddle, Mon. Not. Roy. Astron. Soc. **351**, L49 (2004) doi:10.1111/j.1365-2966.2004.08033.x [astro-ph/0401198].
- [25] H. Jeffreys, *Theory of Probability*, 3rd ed.; Oxford University Press: Oxford, United Kingdom. 1998.
- [26] D. M. Scolnic *et al.*, Astrophys. J. **859** (2018) 101

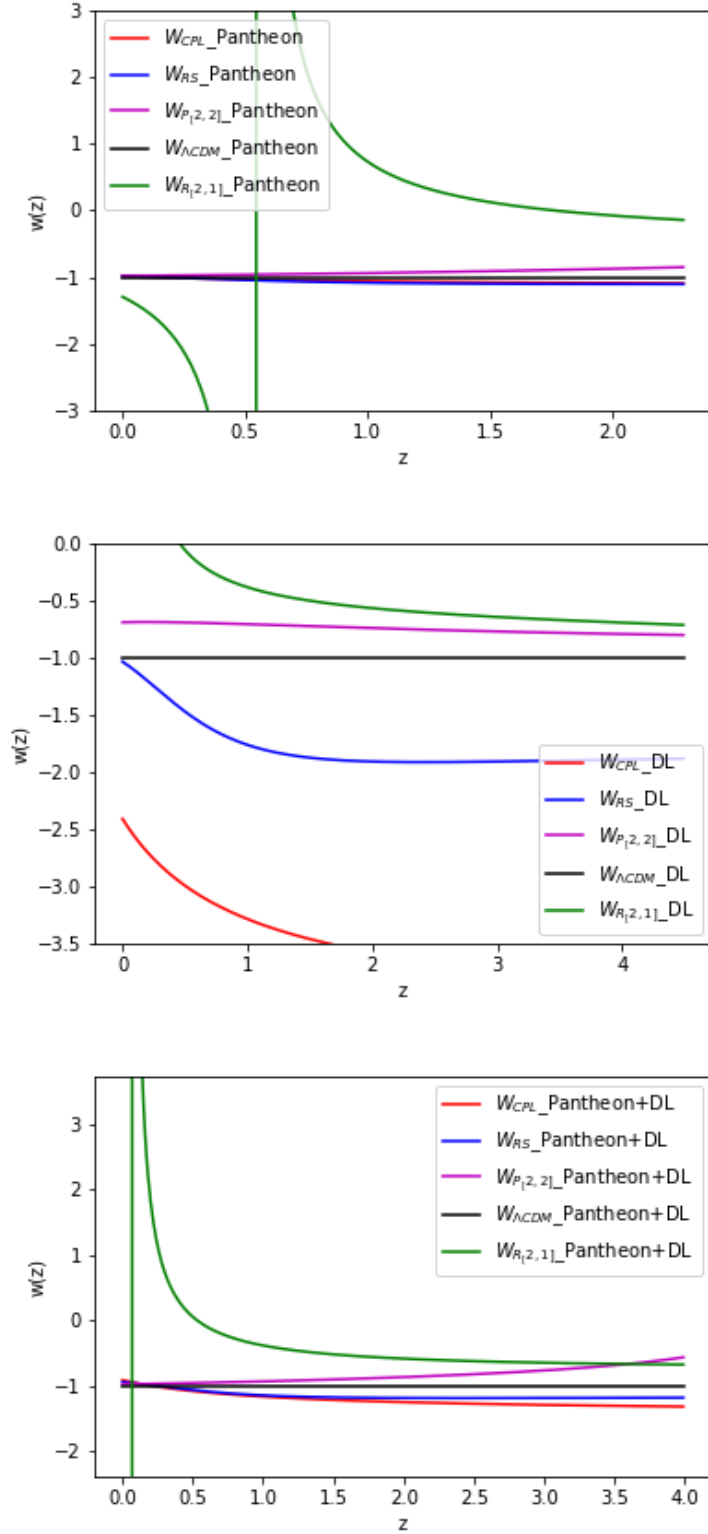


**Figure 15:** Equation of state for the standard cosmological models Sec.(3.1) and  $f(z)$ CDM cosmological models Secs.(3.2-3.3) obtained using the best fits reported for each sampler and cases.  $\Lambda$ CDM model is denote by a solid black line, the standard models CPL and RS by solid red and blue lines, respectively and the Padé (2,2) and Chebyshev (2,1) models by purple and green lines, respectively.